Author Manuscript

Author Manuscript

Author Manuscript

Author Manuscript

HHS Public Access

Author manuscript

J Mol Cell Cardiol. Author manuscript; available in PMC 2022 May 01.

Published in final edited form as:

J Mol Cell Cardiol. 2021 May ; 154: 6–20. doi:10.1016/j.yjmcc.2021.01.001.

Spatial N-glycomics of the Human Aortic Valve in Development and Pediatric Endstage Congenital Aortic Valve Stenosis

Peggi M. Angel[1,*], **Richard R. Drake**[1], **Yeonhee Park**[2], **Cassandra L. Clift**[1], **Connor West**[1], **Savanna Berkhiser**[1], **Gary Hardiman**[4], **Anand S. Mehta**[1], **David Bichell**[3], **Yan Ru Su**[5]

[1]Department of Cell and Molecular Pharmacology; MUSC Proteomics Group; Bruker Clinial Glycomics Center of Excellence, Medical University of South Carolina, Charleston, SC

[2]University of Wisconsin-Madison, Department of Biostatistics and Medical Informatics, Madison WI

[3]Division of Pediatric Cardiac Surgery, Vanderbilt University Medical Center, Nashville, Tennessee

[4]School of Biological Sciences, Queen's University Belfast, United Kingdom

[5]Division of Cardiovascular Medicine, Department of Medicine, Vanderbilt University Medical Center, Nashville, Tennessee

Abstract

Congenital aortic valve stenosis (AS) progresses as an obstructive narrowing of the aortic orifice due to deregulated extracellular matrix (ECM) production by aortic valve (AV) leaflets and leads to heart failure with no effective therapies. Changes in glycoprotein and proteoglycan distribution are a hallmark of AS, yet valvular carbohydrate content remains virtually uncharacterized at the molecular level. While almost all glycoproteins clinically linked to stenotic valvular modeling contain multiple sites for N-glycosylation, there are very few reports aimed at understanding how N-glycosylation contributes to the valve structure in disease. Here, we tested for spatial localization of N-glycan structures within pediatric congenital aortic valve stenosis. The study was done on valvular tissues 0–17 years of age with de-identified clinical data reporting pre-operative valve function spanning normal development, aortic valve insufficiency (AVI), and pediatric endstage AS. High mass accuracy imaging mass spectrometry (IMS) was used to localize N-glycan profiles in the AV structure. RNA-Seq was used to identify regulation of N-glycan related enzymes. The N-glycome was found to be spatially localized in the normal aortic valve, aligning with fibrosa, spongiosa or ventricularis. In AVI diagnosed tissue, N-glycans localized to hypertrophic commissures with increases in pauci-mannose structures. In all valve types, sialic acid (N-acetylneuraminic acid) N-glycans were the most abundant N-glycan group. Three sialylated N-glycans showed common elevation in AS independent of age. On-tissue chemical

[*]Corresponding authors t: 173 Ashley Ave, BSB358, Charleston, SC 29425, angelp@musc.edu.

Disclosures

None.

Publisher's Disclaimer: This is a PDF file of an unedited manuscript that has been accepted for publication. As a service to our customers we are providing this early version of the manuscript. The manuscript will undergo copyediting, typesetting, and review of the resulting proof before it is published in its final form. Please note that during the production process errors may be discovered which could affect the content, and all legal disclaimers that apply to the journal pertain.

Author Manuscript Author Manuscript Author Manuscript Author Manuscript

methods optimized for valvular tissue determined that aortic valve tissue sialylation shows both α2,6 and α2,3 linkages. Specialized enzymatic strategies demonstrated that core fucosylation is the primary fucose configuration and localizes to the normal fibrosa with disparate patterning in AS. This study identifies that the human aortic valve structure is spatially defined by N-glycomic signaling and may generate new research directions for the treatment of human aortic valve disease.

Graphical Abstract

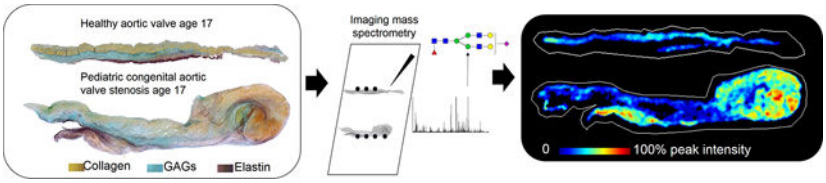

Keywords

aortic valve; congenital aortic valve stenosis; N-glycan; N-glycosylation; extracellular matrix; valve development; imaging mass spectrometry; tissue imaging; MALDI imaging mass spectrometry

INTRODUCTION

Congenital aortic valve stenosis (AS) occurs at an incident rate of over 13.9 in 1000 births, yet there are no medicinal treatments for the disease [1, 2]. AS progresses as an obstructive narrowing of the aorta due to congenital defects that fuse, enlarge and deform the aortic valve (AV) leaflets [3, 4]. Nearly all patients with moderate to severe AS develop left ventricular hypertrophy leading to heart failure [5]. AS has two primary endpoints that are age-dependent, implicating different disease mechanisms [6, 7]. In pediatric endstage AS, excess and disorganized extracellular matrix is deposited within the leaflets leading to pediatric heart failure. In adult endstage AS, leaflets are also enlarged by ECM expansion, but intervention to prevent heart failure is not required until middle age when calcific nodules emerge to restrict heart function [6, 8]. Surgical valve replacement is the only treatment for AS, and for pediatric endstage AS, this is especially detrimental. Pediatric valve replacement devices are limited by their inability to grow with age [9] and increased mortality rates [10]. A major knowledge gap in developing therapies inhibiting pediatric AS is that the molecular mechanisms remain poorly defined. In particular, multiple glycoproteins associated with progression and endstage AS may have N-linked glycans (N-glycan) [11–15], yet these important post-translational modifications remain mostly undefined in human heart valve biology.

N-glycosylation is a complex carbohydrate post-translational modification that modulates protein signaling during development and disease. The N-glycan structure is composed of a series of sugar units created from nucleotidic, metabolic, and translational processing [16–19]. N-glycans attach to the glycoprotein structure at asparagine residues within the consensus sequence NXS/T>>>C, ≠P[20–22]. All eukaryotic N-glycans have a common

Author Manuscript Author Manuscript Author Manuscript Author Manuscript

core of two N-acetylglucosamine (GlcNAc) and three mannose residues [16]. Further sugar units are added through enzymatically driven activities of trimming, branching and capping dependent on biological status [16, 23]. Generally, genetic mutations affecting assembly or initiation of the N-glycan structure are embryonic lethal, whereas mutations associated with trimming, extension, and capping produce variable abnormalities [17]. Disease-mediated alteration of N-glycan structures results in inappropriate cell-cell recognition, migration and proliferation, and disease-enhancing changes along major signaling pathways such as TGFβ1[24–27], JNK[28], ERK[29], EGFR[30], Notch[31].

There are many N-linked glycoproteins that regulate the aortic valve structure and function during development and disease. The glycoproteins tenascin C (TNC), tenascin X precursor (TNXB), Von Willebrand Factor (VWF), and fibronectin 1 (FN1) are regulated with AS progression and all have multiple sites for N-glycosylation [11–15]. Collagens are the main proteins of the valve scaffold [13, 32–35] and all contain consensus sites for N-glycosylation. Numerous studies have reported spatial and cell specific N-glycosylation changes associated with cardiac pathologies [36–43]. However, there are few studies on N-glycan regulation of the aortic valve structure. During normal aortic valve aging, regulation of N-glycosylation was independent of the glycoprotein carriers [44]. This study demonstrated that the normal adult AV from 21–51 years of age has sequential increases in high mannose structures, sialic acids, tri-antennary branching with decreases in core fucosylation. Adult endstage AS has been linked to decreased lumican N-glycosylation with multiple sites of N-glycosylation varying in ECM type proteins [45]. Although it is apparent that dynamic changes in N-glycosylation are important to AV heath and disease, details on N-glycan structure in development or pediatric disease remain unknown.

Spatial regulation of the aortic valve structure is critical for valvular function [35]. During early somatic growth, the AV develops a precise trilayer extracellular matrix structure that becomes deregulated in disease, and this leads to heart failure [4, 35, 46]. However, understanding spatial regulation of N-glycan patterns within the valve structure is an analytical challenge. Conventional studies on N-glycan regulation use liquid chromatography coupled to mass spectrometry [47, 48]. These studies require homogenization of the tissue which eliminates spatial investigations. Imaging mass spectrometry (IMS) is an approach that allows investigation of the spatial localization of molecules within the tissue microenvironment [49–51]. IMS scans across tissue, collecting thousands of x, y datapoints or pixels, each of which report up to thousands of analytes. Each analyte may be visualized as a heatmap of expression across the tissue referenced to tissue features.

Here, we present the first report of N-glycan configuration and regulation involved in pediatric congenital aortic valve stenosis. Pediatric normal and AS valvular tissue sections were probed for N-glycan profiles using high mass accuracy matrix-assisted laser desorption/ionization imaging mass spectrometry (MALDI IMS). N-glycan configuration was evaluated using new technological advances that define N-glycan structural configuration while maintaining spatial references to tissue features. Specifically, an on-tissue chemical modification was optimized to report localization of sialic acid linkages within valve structures [52]. New enzymatic approaches were optimized to define aortic

Author Manuscript Author Manuscript Author Manuscript Author Manuscript

valve N-glycans with core versus branched fucose structures [52]. Parallel RNA-Seq analysis was used to evaluate glycosidase and glycosyltransferase regulation associated with N-glycosylation changes. Our results suggest that N-glycosylation is spatially regulated within the normal valve structure with a dominant core-fucose phenotype, and that pediatric endstage AS involves increases in certain sialylated N-glycans independent of age. This study defines role for N-linked glycosylation in human aortic valve development and childhood disease which may lead to new research directions for the treatment of human heart valve disease.

METHODS

AV Tissue

Tissues were obtained from the Vanderbilt Cardiology Core Laboratory for Translational and Clinical Research (CLTCR) and from the National Disease Research Interchange. The aortic valve tissues were collected under the Vanderbilt Pediatric Congenital Heart Disease Biorepository, written consent was obtained and the project was approved by theVanderbilt Institutional Review Board (IRB) and the IRB at the Medical University of South Carolina. Aortic valves were obtained from excision of leaflet during reparative or transplant surgery, characterized based on de-identified information on AV function, status as bicuspid leaflet or trileaflet, left ventricular wall motion, and extracellular matrix organization by Movat's pentachrome stain. AV function was designated as hemodynamically altered if there was presence of aortic insufficiency or left ventricular wall motion was noted as being significantly altered. Details on tissue preparation are in Supplemental Methods.

Characterization of Collagen, Glycosaminoglycan (GAG) and elastin content

Formalin-fixed, paraffin-embedded (FFPE) tissue was stained with Movat's Pentachrome stain (Polyscientific R&D Corp., Bay Shore, NY, USA). Movat's Pentachrome differentiates ECM components of the leaflets with yellow staining collagens, blue staining glycosaminoglycans (GAGs), black/purple staining elastin and black staining nuclei.. Stained tissue was scanned at 20X using a Miramax slide scanner (Carl Zeiss, Thornwood, NY USA) or an EVOS cell Imaging system (Thermo Fisher Scientific, Waltham, MA). ECM content was characterized segmenting images using ImageJ with the Color Deconvolution plugin (See Supplemental Methods).

Tissue Preparation for Spatially Profiling N-glycoforms

N-glycans were mapped as previously described [53, 54]. Briefly, tissues were heated, dewaxed, antigen retrieved at pH 3 using citraconic anhydride buffer (Thermo Scientific). Tissues were sprayed with PNGase F Prime (N-zyme Scientifics) using an M3 TM-Sprayer (HTX Technologies) with 15 passes at 25 μL/min, 1300 mm/s, 45°C, 3.0 mm spacing between passes with 10 psi nitrogen gas and incubated for 2 hours at 37°C and ≥80% relative humidity. Matrix α-cyano-4-hydroxycinnamic acid (CHCA, Sigma; 50% acetonitrile/0.1% trifluoroacetic acid) was sprayed onto the tissues with an M3 TM-Sprayer (HTX Technologies) using 10 passes at 100 μL/min, 1200 mm/s, 79°C, 2.5 mm spacing between passes and 10 psi nitrogen gas.

Author Manuscript Author Manuscript Author Manuscript Author Manuscript

Core Fucosylated N-glycan Profiles

Detection of core fucosylation was done on a subset of tissue prior to PNGase F digestion using Endo F3 (a kind gift from the Mehta Lab, MUSC). Endo F3 is specific for the cleaving N-glycans with core α−1,6 fucose configuration to the N-acetylglucosamine attached to the protein asparagine residue [52, 55]. Tissue for Endo F3 deglycosylation was prepared with the same protocols as used for PNGase F. EndoF3 released N-glycans were then detected by imaging mass spectrometry as described in the current study with a Δ349.1373 Da loss compared to full length N-glycans released by PNGase F. After imaging mass spectrometry, Endo F3-released N-glycans were removed using a high pH/low pH wash [56], and PNGase F was then sprayed onto tissue as described in preceding paragraphs followed by imaging mass spectrometry detection for detection of the full length N-glycan.

On-Tissue Ethyl Esterification of Sialic Acids

On-tissue ethyl esterification of sialic acids was done as described previously [57] with a minimal modification to the method. Briefly, tissues were heated for 1 hour at 60°C, dewaxed with xylenes and ethanol. Slides with tissue were incubated in 250 mM N-(3-dimethylaminopropyl)-N-ethylcarbodiimide, 500 mM 1-hydroxybenzotriazol in 200 proof ethanol for two hours at 60°C. Tissue were then rinsed again in graded ethanol washes (100% ethanol 3 × 3 minutes, 95% ethanol 1 × 1 minute, 70% ethanol 1 × 1 minute, HYPLC grade water 2 × 3 minutes) followed by antigen retrieval at pH 3.0. PNGase F was applied to detect derivatized N-glycans as previously described.

Lectin Staining

Linkage specific patterns were further visualized by lectins specific to the linkage moiety using chromophore conjugated lectins SNA (Sambucus nigra; Siaα2–6Gal/GalNAc) and SiaFind™ alpha 2,3 specific engineered lectin (Lectenz, LLC). Polysialic acids were detected by anti-polysialic (Abcam ab103036, Abcam, Cambridge, MA). Visualization was done using a 3,3'-Diaminobenzidine kit (Abcam, Cambridge, MA) or fluorophore (Vector Laboratories, Burlingame, CA). Lectin stained tissues detected by DAB were scanned at 20X using a Nanozoomer slide scanner (Hamamatsu Photonics, Bridgewater, NJ). Lectins detected by fluorophore were detected using an EVOS™ microscope (Thermofisher Scientific, Waltham MS).

Imaging Mass Spectrometry

Tissues were imaged using a matrix-assisted laser desorption ionization (MALDI) source coupled to a Fourier Transform Ion Cyclotron Resonance Mass Spectrometer (FT-ICR) (7 Tesla solariX™ Legacy, Bruker Scientific, LLC). Transients of 512k megaword were acquired in broadband positive ion mode over m/z 500–5,000 with a calculated on-tissue mass resolution at full width half maximum of 81,000 at m/z 1400. Lockmass on primary sodiated N-glycan peaks A2G2 (m/z 1663.5814), Man9 (1905.6339) and FA2G2A (2100.7347) was maintained at 15 ppm during tissue imaging. Data were visualized in flexImaging 4.0 and analyzed by SCiLS Lab Pro 2019 (Bruker Scientific, LLC, Bremen, Germany). Images were loaded together and normalized to total ion current. Image segmentation is reported using the Manhattan metric for segmentation. Sodiated

Author Manuscript Author Manuscript Author Manuscript Author Manuscript

N-glycoforms were identified using databases in GlycoworkBench v 2.0[58] to ± 3 ppm mass accuracy. N-glycoform structures are drawn using Glycoworkbench 2.0. Peak areas (imaging data). Exported peak intensities are visualized after natural log transformation with MultiExperiment Viewer (http://www.tm4.org)[59] or ClusterVis[60].

RNA-Seq Data

Tissue preparation is described in Supplemental Methods. Paired end 250 bp (2×125) sequencing was done on a HiSeq2500 sequencer (Illumina, San Diego, CA). Reads were mapped to *Homo sapiens* reference genome with TopHat software [61].Data was processed using OnRamp's advanced Genomics Analysis Engine including data validation and quality control, read alignment to the human genome (hg19) using STAR RNA-seq aligner, generation of gene-level count data with HTSeq [62–64]. Glycosidases and glycosyltransferases were manually curated from log normalized RNA-Seq data.

Statistical Analysis

SSPS version 25 or Graphpad version 8.4.3 were used to calculate Mann-Whitney U (MWU) exact p-values in pairwise comparisons between designated groups. Type I error probability of ≤0.1 was used to evaluate the significance of the result. The p-values of ≤0.1 are reported as trending to significance and ≤0.05 was used determine significant results. Grubb's test for outliers with alpha set to 0.05 was used to test for outliers. Further significance testing was done using one way Kruskal-Wallis ANOVA p-value ≤0.01 corrected for multiple comparisons using the method of Benjamini and Hochberg [65].

RESULTS

Overview.

A collection of 19 aortic valve tissues was tested for localization and regulation of N-glycosylation using novel advances in N-glycomic tissue imaging. We describe the novel technology for glycomics spatial referencing with the results. Data from each tissue includes Movat's pentachrome staining, imaging mass spectrometry data of N-glycans and additional derivatization and endoglycosidase studies accompanied by antibody and lectin staining. Results are shown as 2D images ordered by N-glycosylation synthesis, spanning high mannose (5–9 mannose residues), hybrid N-glycans (combinations of 4 or more mannose residues plus additional sugar residues on branches), and complex N-glycans with variations in sugar residue combinations composing on bi-, tri- and tetra-antennary N-glycans. Core versus branched fucosylation is defined on a subset of high-quality tissue sections. Sialic acid containing N-glycans are presented with chemical derivatization that highlights variation in sialic acid linkages within the human aortic valve structure. Categories of glycoenzymes explored by RNA-Seq in the study are presented in Table 1 [66].

Organization and growth patterns of extracellular matrix from tissue with pediatric congenital aortic valve stenosis are highly individualized.

Movat's pentachrome staining of the samples demonstrated that pediatric endstage AS shows individualized patterns of extracellular matrix (Supplemental Figures 1 & 2). Overall age range spanned 0.15 −17 years of age; not including the Ross pulmonic autograft, mean

Author Manuscript Author Manuscript Author Manuscript Author Manuscript

age was 6.67; 95% CI [3.96, 9.36]. All tissues from pediatric endstage aortic valve stenosis showed bicuspid leaflets and were identified as having stenosis with AVI (Table 2). A failed pulmonic valve with mild stenosis and mixed ECM operating in the aortic position (ROSS) was included to understand the potential for pathological variation related to ROSS failure. To summarize, the clinical cohort showed typical variation in extracellular matrix patterning suitable for characterizing N-glycan expression in pediatric endstage aortic valve stenosis.

N-glycans represent an abundant and complex post-translational modification within the human aortic valve.

Tissue imaging glycomics [54, 67, 68] uses the enzyme PNGase F to target and hydrolyze the N-glycans from proteins, cleaving between the terminal core N-acetylglucosamine (GlcNAc) and the asparagine residue of the protein backbone. The enzymatic approach is highly specific to N-glycans, unbiased to N-glycan structure and leaves the N-glycans intact and localized to tissue microregions. A total of 123 N-glycans were mapped across 19 aortic valve tissues (Fig. 1, Supplemental Table 1). Fig. 2A demonstrates the types of N-glycn structures found by the study. Sialylated N-glycans (N-acetylneuraminic acid, NeuAc) represented the largest group of N-glycans detected over all tissues (54 N-glycans, 44% of the total N-glycan profile) (Fig. 1B). Tri- and tetra-antennary N-glycans with NeuAc were consistently detected in all valvular tissues. Fucosylation without sialylation represented a significant group (38 N-glycans, 31% of the total N-glycan profile). Fucosylated and highly branched N-glycans represented the second and third largest group detected in human aortic valve tissue (16 N-glycans (13% of the total N-glycan profile and 14 N-glycans, 11% of the total N-glycan profile, respectively). Spectral comparison of age-matched individuals having normal AV or with AS demonstrated that both tissue types have complex N-glycan profiles (Fig. 1B). The bi-antennary fucosylated N-glycan at m/z 1809.6393 (m/z 1809) was the most abundant peak by intensity in all AV tissue regardless of age and disease status; this was characterized as a primary N-glycan signature of the human aortic valve (Fig. 1C). Overall, the data demonstrated that the N-glycome profile of the human aortic valve is significantly comprised of sialylated and fucosylated species.

The thickened free edge shows increases in specific N-glycans.

Image segmentation was done to determine primary patterns of N-glycosylation within aortic valve structures. Image segmentation uses hierarchical clustering to group N-glycan peaks by intensity and localization within the tissue. Segmentation patterns give a spatial reference to unique N-glycomes within the tissue (Fig 2A, Supplemental Figure 3). N-glycomic patterns generally localized to patterns of ECM observed in the valve structures. Analysis of N-glycome clusters localized to the thickened free edge in certain tissues (white arrows, Fig. 2A) showed that five specific N-glycans could sensitively and specifically differentiate the pathologically thickened free edges compared to the medial portion (or belly) of the valve (Fig. 2B, Supplemental Methods). Elevation of the same N-glycome was also present in the thickened free edge of the failed pulmonic valve that had been placed in the aortic position by Ross procedure. To conclude, N-glycan spatial patterns show that N-glycans follow gross ECM patterning across the aortic valve structure with distinctive regulation at pathological sites, particularly the thickened free edge.

Author Manuscript Author Manuscript Author Manuscript Author Manuscript

Phenotypes of Aortic Valve Insufficiency Show Altered N-glycosylation.

A subset of N-glycans were identified that were altered by AVI (Fig. 3). These included paucimannose N-glycans M2, M3 (where M is the number of mannose residues present (Figs. 3 A–C, **respectively**) that were significantly elevated throughout AVI tissues compared to normal or AS tissues. However, as complexity of the N-glycans increased, certain N-glycans decreased relative to AVI. This included Man4 (Fig. 3D), bi-antennary abundant N-glycan 1809 (Fig. 3E), tri-antennary branching (Fig. 3F, G) or tetra-antennary structures (Fig 3H, I). These data suggest that valvular mechanics may influence N-glycosylation and infer transitions in N-glycan regulation relevant to progression of valvular dysfunction.

High Mannose N-Glycans Localize Primarily to Collagenous Regions.

To understand initial steps of N-glycosylation, high mannose and hybrid structures were analyzed. Spatial analysis showed that in normal valves, mannose structures aligned with the fibrosa layer while in AS the expression pattern was intense and diffuse throughout the structure (Fig. 4A, Supplementary Table 1). For normal valves, a significant age-related decrease was detected in the ratio of Man8 (glycoprotein folding) to Man5 (mannose trimming prior to extension) (Spearman's correlation −0.95, p-value 0.048, Supplemental Figure 4), suggesting a progression of N-glycan activity throughout childhood development. Ratios of Man8 to Man5 in AS remained constant across pediatric age groups (1.24 ± 0.55, ANOVA p-value 0.31). Interestingly, a significant increase was detected in AS levels of Hex5HexNAc3 +Na, m/z 1460.5020 (m/z 1460) compared to normal valves (Fig. 4B; MWU p-value 0.049). This structure represents a transition between trimming and addition of GlcNAc for branching[16, 69, 70], suggesting that in AS there may be incomplete processing of N-glycan structure. Spatial mapping showed that m/z 1460 had low levels of expression in the young normal valve structures (Fig. 4C). In AS, m/z 1460 increased throughout the valve structure (Fig. 4D). Overall, these data report that initial steps of N-glycan processing are a localized and active phenemona in human aortic valves that spatially change with disease patterns.

Core Fucosylation Is a Primary Fucose Configuration of Aortic Valve N-Glycans.

Core α1,6 fucosylation is a critical N-glycan modification that has been reported to drive TGFβ pathways and decreases in core fucosylation may attenuate fibrosis [24, 26]. To understand the fucose configuration of the human aortic valves, a subset of AV tissues was probed to determine fucose status. The strategy used the Endo F3 endoglycosidase, which targets the core fucosylation and not branched fucosylation, from tissue [52] (Figure 5A). In normal valves, the number of core fucosylated N-glycans was nearly three times higher in the fibrosa versus the spongiosa (Figure 5B). Furthermore, principal components analyses on spectra from normal fibrosa or spongiosa demonstrated that the spectra generated containing core fucosylation separate distinctly based on localization to fibrosa or spongiosa within the aortic valve structure (Figure 5C). Multiple core fucosylated N-glycans showed precise localization with the fibrosa in normal AV tissue as young as 2 years of age (Figure 5D). A single bi-antennary, core-fucosylated sialylated N-glycan m/z 1611.5257 was localized to the spongiosa and not the fibrosa. The most abundant N-glycan in all AV

Author Manuscript Author Manuscript Author Manuscript Author Manuscript

tissue was Hex5dHex1HexNAc4 + 1Na, m/z 1809.6393 (m/z 1809) and this N-glycan was detected as being primarily core-fucosylated in human aortic valve tissue. AS demonstrated primarily a core-fucosylated phenotype (Figures 5E–G). In a single patient with an AS endpoint at age 2 weeks, the phenotype was reversed with high expression patterns of branched fucosylation (Figure 5E SKU 0.04-B-S-AVI). Combined ion mapping highlighted potential pathological localization patterns of fucose N-glycans within the AV structure (Figure 5H). Here, a double sialylated tri-antennary core fucose aligned with spongiosa in the normal AV but showed disparate patterning in AS structure that did not overlap with the primary core-fucosylated N-glycan m/z 1809. These findings provide evidence that localized regulation of core fucosylation is a primary N-glycan pathway within the human aortic valve and may be deregulated in pediatric endstage AS.

NeuAc Containing N-Glycans with Specific Linkage Patterns are Elevated in Pediatric Endstage AS.

The sialic acid N-acetylneuraminic acid (NeuAc) is a terminal addition to the N-glycan and sialic acid N-glycan regulation in human biology plays a large role in cell-cell and cell-ECM interactions, including immune cell interactions [71–73]. Sialylated NeuAc N-glycans represented the most abundant population of N-glycans in the human aortic valve. Quantification of NeuAc N-glycans showed that very specific N-glycans were elevated in end stage AS independent of age (Fig 6A–C, Supplemental Figure 5). These included the bi-antennary N-glycan 1976.6566 (m/z 1976, Fig. 6A), the fucosylated N-glycan m/z 2163.7511(m/z 2163 Fig. 6B), and the tri-antennary N-glycan m/z 2341.7998 (m/z 2341, Fig. 6C). A common localization motif was the presence of these N-glycans within the older valves that had thickened commissures, including the ROSS pulmonic valve operating in the aortic valve position. On-tissue chemical derivatization was done to understand α2,3 and α2,6 linkage specificity of NeuAc per patient. The m/z 1976 was primarily α2,6 linked (Fig. 6D) with younger AS ≤ 5 yrs demonstrating a 20% relative abundance of α2,3 linkages. The m/z 2163 was also primarily α2,6 linked, yet had suggestive age-related decreases of α2,3 linkage (Fig. 6E). However, the m/z 2341 showed high relative ratios of α2,3 linkage with minimal presence of α2,6 linked NeuAc (Fig. 6F). Localization of specific linkages types showed co-localized with primarily with regions that contained mixed elastin by Movat's pentachrome staining (Fig 6G, I). Carbohydrate binding lectins, which bind to all N-glycans containing a specific motif and configuration of several sugars, were used to to further confirm the existence of differentially localized NeuAc linkages. Lectin staining by *Sambucus nigra agglutin* (high affinity for α2,6 NeuAc-galactose-GlcNAc motif) also showed that α2,6 localized to regions of elastin mixing (Fig. 6H). A lectin specific to the α2,3 NeuAc--galactose- GlcNAc motif demonstrated similar patterning with more intense staining in the elastin rich regions (Fig. 6J). These data are suggestive that regulation of certain sialiylated N-glycans with specific linkages may play a pathological role in the elastin-collagen deregulation of AS.

The Human Aortic Valve Shows Active Transcriptional Regulation of Sialic Acid Glycosidases, Glycosyltransferases and Siglecs.

Since sialic acids were the most abundant N-glycan in the human aortic valve with significant AS regulation, the RNA-Seq data was evaluated for transcriptional expression

Author Manuscript Author Manuscript Author Manuscript Author Manuscript

patterns of neurominidases, sialyltransferases, and sialic acid-binding immunoglobin-type lectins (Siglecs). In general, the individual valve tissues demonstrated unique patterns of transcriptional levels related to sialic acid (Fig 7A, Supplemental Table 2). Generally, Sialic acid-binding Ig-like lectins (Siglecs) were found to be increased in AVI (Fig. 7A). Sialic acid binding Ig-like lectin (SIGLEC12), a controversial adhesion regulator suggested to recruit SHP1 and SHP2 through adhesion binding to epithelial cells[74, 75], increased in AS (3.9-fold AS/Normal, MWU p-value 0.036). Interestingly, neuraminidases, which cleave terminal sialic acids from glycoproteins and glycolipids, showed negligible variation in transcript level across all valve tissues (Fig. 7B). Relative abundance levels of neuraminidases in both normal and disease valves were Neu1 (46.2 ± 1.8% abundance), Neu3 (37.1 ± 1.6%), Neu4(16.7 ± 3.2%). Neu2 transcription levels were not detected in human aortic valve. Finally, transcripts related to α2,8 polysialic acid addition were detected in all pediatric aortic valves with patient-specific variation in expression levels. This was surprising since reports in rat models of heart development show that polysialylation is precisely regulated in the outflow tract and decreases post-transitional circulation[76]. To further understand localization of polysialylation in AS, valve tissue was stained for ST8SIA4 enzyme (Fig. 7D, Supplemental Figure 6). ST8SIA4 was primarily detected in the valvular endothelium with ST8SIA4 positive cells in the fibrosa of normal valves and in valvular interstitial cells throughout the pediatric AS structure. Regulation of sialylated N-glycans remains active at the transcriptional and glycomic level in AS valvular tissue, yet may lead to common structural endpoints of disease.

Discussion

N-glycosylation is developmentally regulated and disease altered within the human aortic valve structure. Our study found that the trilayer structure of the normal valve is defined by very specific N-glycan structures. In AS, N-glycans are not only altered by abundance and configuration but also show distinct spatial patterns throughout the valvular structure. Spatial patterns may attributable to cellular phenotypes or changes in metabolism as part of the underlying congential disease. Glycosylation is an effector of cell-ECM and cell-cell interactions that are critical to maintaining the aortic valve structure [17, 77]. Various subtypes of valvular interstitial cells (VIC) exist within the valvular structure alter the valvular structure-function relationship through abnormal ECM production [78, 79] and pathological N-glycosylation contributes to abnormal cell-ECM interactions [80, 81]. Incorrect glycosyation may induce aberrant endothelial mesenchymal transition (EMT) [82–84] through inappropriate activation of the hexosamine biosynthetic pathway. Specific inborn errors of metabolism influence protein and lipid glycosylation to result in dysplastic and bicuspid valve defects [85].

A significant and novel finding was that the young human aortic valve shows (α1,6) core-fucosylated N-glycans as the primary type of fucosylation. Core fucosylation regulates valvular signaling pathways, such as NOTCH, E-cadherin, TGFβ1, EGFR that are critical regulators of structure [30, 86–88]. Research on fibrotic disease shows that core fucosylation of TGFβ1 activates EMT and leads to overproduction of collagen [24, 87, 89]. Although core fucosylation regulates EMT in many human cancers mainly through TGFβ pathways [90–94], the role of core fucosylation in human valve development and

Author Manuscript Author Manuscript Author Manuscript Author Manuscript

valvular fibrosis is unknown. Attenuation of core-fucosylation has been shown to be a viable approach to reduce disease mediated EMT, limit excess collagen production and reduce the inflammatory response [26, 95, 96]. As examples, inhibition of core fucosylation through FUT8 deletion inhibited TGFβ2 and ALK5 expression to decrease renal fibrosis [24]. In calcific vascular smooth muscle cells siRNA inhibition of FUT8 decreased core fucosylation and effectively blocked TGFβ1/Smad2/3 signaling activation [43]. Immune cell activation and reduce autoinflammatory diseases were reduced by loss of core fucosylation [97]. Interestingly, previous research has shown that in the healthy adult AV, fucosylation decreases with age [44]. Fucosylation, and particularly core fucosylation, may be a route for control and regulation of the aortic valve structure that contributes to deregulation of pediatric AS.

The study identified that N-glycans with the sialic acid N-acetylneuraminic acid represented the majority of the young human aortic valve N-glycome. Broadly speaking, sialic acid expression is very complex, with variation in linkage to the terminal galactose as well as additional modifications within the sialic acid structure [73, 98]. A main role for sialic acid N-glycans are to control cell-cell and cell-ECM interactions first through the negatively charged and hydrophilic sialic acid, then through conformational changes required for ligand binding based on linkage type [73, 98]. Linkage variation is dependent on cell type and can dramatically alter the recruitment of cells during development or modulate immune response during development or disease [73, 99, 100]. In cardiomyocytes, increases in sialylation of N-glycoproteins by cardiac hypertrophy has been attributed to increased protein synthesis along pathways of wound healing, cell adhesion and inflammatory response [37]. Endothelial sialylation turnover is sensitive and rapid, occurring within hours of proinflammatory stimulation to increase leukocyte recruitment [101]. Further studies are needed to demonstrate a role for sialic acid N-glycans in the pediatric AS immune response.

Regulation of sialylation was found also found at the transcriptional and translational levels in young valves. Sialyltransferases have been implicated in cancer with a tissue dependent role in invasiveness and metastasis [102, 103], potentially translating to AS problems of inappropriate migration and differentiation [4, 104] that could also be hemodynamically influenced [105]. ST8SIA4, a sialyltransferase that adds consecutive α2,8 sialic acids carried by NCAM, is developmentally down regulated in the outflow tract post-transitional circulation [76, 106]. The finding of ST8SIA4 positive endothelial and VIC cells within AS tissue up to 17 years of age is a novel observation that could suggest a prolonged developmental program or could arise from ongoing poor hemodynamics; it will be critical to identify the α2,8 sialic acids glycoprotein carriers. The study also identified Siglecs involved in the pediatric valve. Siglecs are primarily expressed by immune cells with a role in negative immune modulation through sialic acid binding [107–109]; mutation of the SIA binding site may prevent or allow only weak sialic acid binding by Siglec-12 [74, 110]. Siglec-12, shown here to be increased in AS, is expressed not only on macrophages but also luminal epithelial surfaces in humans and chimpanzees [74, 75].

This study provides evidence that localization of N-glycans may be affected by valvular hemodynamics and this may play a role in diagnostic valve function. Localization to valvular subanatomy such as the commissure, collagenous fibrosa, glycosaminoglycan-rich

Author Manuscript Author Manuscript Author Manuscript Author Manuscript

spongiosa, and elastic ventricularis suggest that very specific N-glycan distributions are required for appropriate valvular function. Contemporary literature shows that N-glycan expression in cultured cells is altered by hemodynamics and, in vascular structures, is a known effector of adhesion expression changes with a role in modulating immune recruitment [101, 111, 112]. In atherogenic endothelial cells, oscillatory shear resulted in hyperglycosylation due to increases in high mannose structure, reducing monocyte recruitment by restricting further processing of N-glycosylation [113]. Congenital defects of N-glycosylation frequently involve cardiovascular defects with a consequence of altered hemodynamics [36, 114]. The overall evidence suggests that the valvular hemodynamic signaling exchange includes contributions from localized regulation of N-glycosylation. To support this concept, additional imaging experiments over an entire rat heart showed that the hemodynamically differing regions of the aortic valves and outflow tract have very distinctive regulation of N-glycans (Supplemental Figure 7). N-glycan signaling altered by hemodynamics may feed forward into cell-cell, cell-immune cell, and cell-matrix interactions that further affect the structural integrity and function of the valve [17, 115].

This study had limitations. Normal valve tissue from pediatric ages are challenging to obtain as parents may be less likely to donate pediatric tissues to transplant or scientific study [116]. Certain normal functioning valve tissues used in the study were from failed hearts with an unknown impact on valve biology. In spite of unknowns, the tissue classified by normal function, AS or altered hemodynamics appears to group closely by N-glycan profiles. The normal AV tissue available to the study spanned the age range of post-transitional pediatric growth patterns (age 0–17). Not all of the valvular tissue was available for each portion of the study. This led to a limited understanding of certain N-glycan configurations and glyco-enzyme regulation that could be linked to disease. The study was able to report patient specific regulation in glyco-enzymes and found that certain N-glycan configurations may be common endpoints of AS, independent of age. Finally, the study blindly selected AS tissue from the available tissue bank and it is possible that the pathological variation in ECM from our cohort does not correspond to large populations. The selected cohort provided a wide variety of pathological variation within the aortic valve that was an asset in detailing the N-glycome in valvular spatial organization and this data is driving new hypotheses on N-glycosylation in human aortic valve development and disease.

Conclusion

One of the greatest challenges in understanding heart valve biology is that structure regulates function and function feeds back to regulate structure. Molecular regulation across the valvular subanatomy is thus critical to integrity of the valve structure and heart function. New ‘Omics methods for spatial referencing have been developed within the last decade that may be used to test and report molecular regulation in combination with hemodynamics in single cells, humans and animal models [49, 67, 117–119]. The current study focused on understanding spatial N-glycomics, which spans multiple molecular levels of control. N-glycomic expression requires metabolic regulation in synthesis of sugar units, transcriptional control of enzymes, post-translational control of protein signaling through glycoprotein folding and secretion and post-translational miRNA gene regulation [16, 19, 115]. Numerous therapeutics exist that can block synthesis of particular N-glycans and

Author Manuscript Author Manuscript Author Manuscript Author Manuscript

consequently signaling [120, 121]. An overall finding of the current study was that AS and non-stenotic valve tissue show independent N-glycomic regulation at both transcriptomic and glycomic levels. Much detail remains unknown. Currently undefined are the aortic valve glycoproteins carrying the reported N-glycan structures, target N-glycoprotein site occupancy and impact of N-glycan structure variation at a specific location in the valve and how these data change, if at all, during developmental hemodynamics. There is a lack of understanding on which cells contribute to N-glycan alteration and how cell-specific expression patterns intersect with immune pathways and regulation of aortic valve maturation. However, the exacting spatial distribution of the N-glycome strongly suggests a significant role in regulation of the human aortic valve in development and disease. The techniques developed for the study provide the foundational approaches for N-glycomic investigation of valvular disease across all mammalian species. This study establishes that the N-glycome aligns with the human aortic valve structural features that are necessary for appropriate valve function and are subsequently delocalized and deregulated by AS.

Supplementary Material

Refer to Web version on PubMed Central for supplementary material.

Acknowledgements

Funding provided specifically for this work by the American Heart Association (16GRNT31380005) to PMA with additional support by the NIH/NIGMS (P20 GM103542) and National Center for Advancing Translational Sciences UL1 TR000445, which supported initial studies for the project. PMA is enormously grateful to HSB for early career mentoring on valve development and biology. CLC supported by HL007260 (NIH/NHLBI). Support to RRD provided NCI/IMAT (1R21CA207779) and by the South Carolina Centers of Economic Excellence SmartState program.

Abbreviations:

AS	Aortic valve stenosis
AVI	aortic valve insufficiency
GAG	glycosaminoglycan
HA	hemodynamically altered
Ross	Ross procedure
ECM	extracellular matrix protein
PTM	post-translational modification
MALDI IMS matrix	assisted laser desorption /ionization imaging mass spectrometry
HRAM	high resolution accurate mass
Man	mannose
GlcNAc N	acetylglucosamine

Author Manuscript Author Manuscript Author Manuscript Author Manuscript

NeuAc	N-acetylneuraminic acid

References

[1]. Hoffman JIE, Kaplan S, The incidence of congenital heart disease, Journal of the American College of Cardiology 39(12) (2002) 1890–1900. PMID:12084585. [PubMed: 12084585]

[2]. Hoffman JIE, Kaplan S, Liberthson RR, Prevalence of congenital heart disease, The American Heart Journal 147(3) (2004) 425–439. PMID:14999190. [PubMed: 14999190]

[3]. Moreno PR, Astudillo L, Elmariah S, Purushothaman K, Purushothaman M, Lento PA, Sharma SK, Fuster V, Adams DH, Increased macrophage infiltration and neovascularization in congenital bicuspid aortic valve stenosis, The Journal of Thoracic and Cardiovascular Surgery 142(4) (2011) 895–901.PMID:21481422. [PubMed: 21481422]

[4]. Hinton RB Jr, Lincoln J, Deutsch GH, Osinska H, Manning PB, Benson DW, Yutzey KE, Extracellular matrix remodeling and organization in developing and diseased aortic valves, Circulation Research 98(11) (2006) 1431–1438. PMID:16645142. [PubMed: 16645142]

[5]. Graham TP, Driscoll DJ, Gersony WM, Newburger JW, Rocchini A, Towbin J, A., Task Force 2: Congenital Heart Disease, Journal of the American College of Cardiology 45(8) (2005) 1326–1333. PMID:15837282. [PubMed: 15837282]

[6]. Siu SC, Silversides CK, Bicuspid aortic valve disease, Journal of the American College of Cardiology 55(25) (2010) 2789–2800.PMID:20579534. [PubMed: 20579534]

[7]. Wirrig EE, Hinton RB, Yutzey KE, Differential expression of cartilage and bone-related proteins in pediatric and adult diseased aortic valves, Journal of Molecular and Cellular Cardiology 50(3) (2011) 561–569. PMID:21163264, PMCID: PMC3035730. [PubMed: 21163264]

[8]. Otto CM, Prendergast B, Aortic-valve stenosis—from patients at risk to severe valve obstruction, New England Journal of Medicine 371(8) (2014) 744–756.PMID: 25140960.

[9]. Henaine R, Roubertie F, Vergnat M, Ninet J, Valve replacement in children: A challenge for a whole life, Archives of Cardiovascular Disease 105(10) (2012) 517–528. PMID:23062483.

[10]. McCrindle BW, Blackstone EH, Williams WG, Sittiwangkul R, Spray TL, Azakie A, Jonas RA, Are Outcomes of Surgical versus Transcatheter Balloon Valvotomy equivalent in neonatal critical aortic stenosis?, Circulation 104(suppl 1) (2001) I-152–I-158. PMID:11568048. [PubMed: 11568048]

[11]. Satta J, Melkko J, Pöllänen R, Tuukkanen J, Pääkkö P, Ohtonen P, Mennander A, Soini Y, Progression of human aortic valve stenosis is associated with tenascin-C expression, Journal of the American College of Cardiology 39(1) (2002) 96–101. PMID: 11755293. [PubMed: 11755293]

[12]. Vincentelli A, Susen S, Le Tourneau T, Six I, Fabre O, Juthier F, Bauters A, Decoene C, Goudemand J, Prat A, Acquired von Willebrand syndrome in aortic stenosis, New England Journal of Medicine 349(4) (2003) 343–349. PMID: 12878741.

[13]. Stephens EH, Chu CK, Grande-Allen KJ, Valve proteoglycan content and glycosaminoglycan fine structure are unique to microstructure, mechanical load and age: Relevance to an age-specific tissue-engineered heart valve, Acta Biomaterialia 4(5) (2008) 1148–1160. [PubMed: 18448399]

[14]. Della Corte A, Quarto C, Bancone C, Castaldo C, Di Meglio F, Nurzynska D, De Santo LS, De Feo M, Scardone M, Montagnani S, Spatiotemporal patterns of smooth muscle cell changes in ascending aortic dilatation with bicuspid and tricuspid aortic valve stenosis: Focus on cell–matrix signaling, The Journal of Thoracic and Cardiovascular Surgery 135(1) (2008) 8–18. PMID: 18179910. [PubMed: 18179910]

[15]. Matsumoto K-I, Satoh K, Maniwa T, Araki A, Maruyama R, Oda T, Noticeable decreased expression of tenascin-X in calcific aortic valves, Connective Tissue Research 53(6) (2012) 460–468. PMID: 22827484. [PubMed: 22827484]

[16]. Stanley P, Schachter H, Taniguchi N, Chapter 8: N-Glycans, in: Varki A, Cummings RD, Esko JD, Freeze HH, Stanley P, Bertozzi CR, Hart GW, Etzler ME (Eds.) Essentials of Glycobiology, Cold Spring Harbor Laboratory Press, Cold Spring Harbor (NY), 2009.

Author Manuscript Author Manuscript Author Manuscript Author Manuscript

[17]. Varki A, Freeze HH, Vacquier VD, Chapter 38: Glycans in Development and Systemic Physiology, in: Varki A, Cummings RD, Esko JD, Freeze HH, Stanley P, Bertozzi CR, Hart GW, Etzler ME (Eds.) Essentials of Glycobiology. 2nd edition., Cold Spring Harbor (NY), 2009.

[18]. Bieberich E, Synthesis, processing, and function of N-glycans in N-glycoproteins, Glycobiology of the Nervous System, Springer 2014, pp. 47–70.

[19]. Kasper BT, Koppolu S, Mahal LK, Insights into miRNA regulation of the human glycome, Biochemical and biophysical research communications 445(4) (2014) 774–779. [PubMed: 24463102]

[20]. Marshall RD, The nature and metabolism of the carbohydrate-peptide linkages of glycoproteins, Biochem Soc Sym, 1974, pp. 17–26.

[21]. Lowenthal MS, Davis KS, Formolo T, Kilpatrick LE, Phinney KW, Identification of novel N-glycosylation sites at noncanonical protein consensus motifs, Journal of Proteome Research 15(7) (2016) 2087–2101. [PubMed: 27246700]

[22]. Bause E, Structural requirements of N-glycosylation of proteins. Studies with proline peptides as conformational probes, Biochemical Journal 209(2) (1983) 331–336.

[23]. Moremen KW, Tiemeyer M, Nairn AV, Vertebrate protein glycosylation: diversity, synthesis and function, Nature Reviews Molecular Cell Biology 13(7) (2012) 448–462. [PubMed: 22722607]

[24]. Shen N, Lin H, Wu T, Wang D, Wang W, Xie H, Zhang J, Feng Z, Inhibition of TGF-β1-receptor posttranslational core fucosylation attenuates rat renal interstitial fibrosis, Kidney International 84(1) (2013) 64–77. PMID: 23486519. [PubMed: 23486519]

[25]. Li L, Shen N, Wang N, Wang W, Tang Q, Du X, Carrero JJ, Wang K, Deng Y, Li Z, Inhibiting core fucosylation attenuates glucose-induced peritoneal fibrosis in rats, Kidney International 93(6) (2018) 1384–1396. [PubMed: 29571940]

[26]. Lin H, Wang D, Wu T, Dong C, Shen N, Sun Y, Sun Y, Xie H, Wang N, Shan L, Blocking core fucosylation of TGF-β1 receptors downregulates their functions and attenuates the epithelial-mesenchymal transition of renal tubular cells, American Journal of Physiology-Renal Physiology 300(4) (2011) F1017–F1025. [PubMed: 21228108]

[27]. Tu C-F, Wu M-Y, Lin Y-C, Kannagi R, Yang R-B, FUT8 promotes breast cancer cell invasiveness by remodeling TGF-β receptor core fucosylation, Breast Cancer Research 19(1) (2017) 111. PMCID: PMC5629780. [PubMed: 28982386]

[28]. de Vreede G, Morrison HA, Houser AM, Boileau RM, Andersen D, Colombani J, Bilder D, A Drosophila tumor suppressor gene prevents tonic TNF signaling through receptor N-glycosylation, Developmental Cell 45(5) (2018) 595–605. [PubMed: 29870719]

[29]. Kovács K, Decatur C, Toro M, Pham DG, Liu H, Jing Y, Murray TG, Lampidis TJ, Merchan JR, 2deoxy-glucose downregulates endothelial AKT and ERK via interference with N-Linked glycosylation, induction of endoplasmic reticulum stress, and GSK3β activation, Molecular Cancer Therapeutics 15(2) (2016) 264–275. [PubMed: 26637370]

[30]. Wang X, Gu J, Ihara H, Miyoshi E, Honke K, Taniguchi N, Core fucosylation regulates epidermal growth factor receptor-mediated intracellular signaling, J Biol Chem 281(5) (2006) 2572–2577. PMID: 16316986. [PubMed: 16316986]

[31]. Allam H, Johnson BP, Zhang M, Lu Z, Cannon MJ, Abbott KL, The glycosyltransferase GnT-III activates Notch signaling and drives stem cell expansion to promote the growth and invasion of ovarian cancer, J Biol Chem 292(39) (2017) 16351–16359. [PubMed: 28842505]

[32]. Shapiro S, Endicott S, Province M, Pierce J, Campbell E, Marked longevity of human lung parenchymal elastic fibers deduced from prevalence of D-aspartate and nuclear weapons-related radiocarbon, Journal of Clinical Investigation 87(5) (1991) 1828.

[33]. Balasubramanian S, Johnston RK, Moschella PC, Mani SK, Tuxworth J, William J, Kuppuswamy D, mTOR in growth and protection of hypertrophying myocardium, Cardiovascular & Hematological Agents in Medicinal Chemistry (Formerly Current Medicinal Chemistry-Cardiovascular & Hematological Agents) 7(1) (2009) 52–63.

[34]. Dupuis LE, McCulloch DR, McGarity JD, Bahan A, Wessels A, Weber D, Diminich AM, Nelson CM, Apte SS, Kern CB, Altered versican cleavage in ADAMTS5 deficient mice; A novel etiology of myxomatous valve disease, Developmental biology 357(1) (2011) 152–164. PMID:21749862. [PubMed: 21749862]

Author Manuscript Author Manuscript Author Manuscript Author Manuscript

[35]. Schoen FJ, Evolving concepts of cardiac valve dynamics: the continuum of development, functional structure, pathobiology, and tissue engineering, Circulation 118(18) (2008) 1864–1880. PMID:18955677. [PubMed: 18955677]

[36]. Gehrmann J, Sohlbach K, Linnebank M, Böhles H-J, Buderus S, Kehl HG, Vogt J, Harms E, Marquardt T, Cardiomyopathy in congenital disorders of glycosylation, Cardiology in the Young 13(4) (2003) 345–351. [PubMed: 14694955]

[37]. Rong J, Han J, Dong L, Tan Y, Yang H, Feng L, Wang Q-W, Meng R, Zhao J, Wang S-Q, Glycan imaging in intact rat hearts and glycoproteomic analysis reveal the upregulation of sialylation during cardiac hypertrophy, Journal of the American Chemical Society 136(50) (2014) 17468–17476. [PubMed: 25313651]

[38]. Gudelj I, Lauc G, Protein N-Glycosylation in Cardiovascular Diseases and Related Risk Factors, Current Cardiovascular Risk Reports 12 (2018) 1–11.

[39]. Zhang R, Wang Y, Chen L, Wang R, Li C, Li X, Fang B, Ren X, Ruan M, Liu J, Reducing immunoreactivity of porcine bioprosthetic heart valves by genetically-deleting three major glycan antigens, GGTA1/β4GalNT2/CMAH, Acta biomaterialia 72 (2018) 196–205. [PubMed: 29631050]

[40]. Yin X, Wanga S, Fellows AL, Barallobre-Barreiro J, Lu R, Davaapil H, Franken R, Fava M, Baig F, Skroblin P, Glycoproteomic analysis of the aortic extracellular matrix in Marfan patients, Arteriosclerosis, Thrombosis, and Vascular Biology 39(9) (2019) 1859–1873.

[41]. Ednie AR, Deng W, Yip K-P, Bennett ES, Reduced myocyte complex N glycosylation causes dilated cardiomyopathy, The FASEB Journal 33(1) (2019) 1248–1261. [PubMed: 30138037]

[42]. Ashwood C, Waas M, Weerasekera R, Gundry RL, Reference glycan structure libraries of primary human cardiomyocytes and pluripotent stem cell-derived cardiomyocytes reveal cell-type and culture stage-specific glycan phenotypes, Journal of Molecular and Cellular Cardiology 139 (2020) 33–46. [PubMed: 31972267]

[43]. Wen X, Liu A, Yu C, Wang L, Zhou M, Wang N, Fang M, Wang W, Lin H, Inhibiting post-translational core fucosylation prevents vascular calcification in the model of uremia, The International Journal of Biochemistry & Cell Biology 79 (2016) 69–79. [PubMed: 27521658]

[44]. Przybyło M, Stępień E, Pfitzner R, Lityńska A, Sadowski J, Age effect on human aortic valvular glycoproteins, Archives of Medical Research 38(5) (2007) 495–502. PMID: 17560454. [PubMed: 17560454]

[45]. Suzuki H, Chikada M, Yokoyama MK, Kurokawa MS, Ando T, Furukawa H, Arito M, Miyairi T, Kato T, Aberrant glycosylation of lumican in aortic valve stenosis revealed by proteomic analysis, International Heart Journal 57(1) (2016) 104–111. [PubMed: 26742884]

[46]. Merryman WD, Schoen FJ, Mechanisms of calcification in aortic valve disease: role of mechanokinetics and mechanodynamics, Current Cardiology Reports 15(5) (2013) 1–7. PMCID: PMC3658606

[47]. Dong X, Huang Y, Cho BG, Zhong J, Gautam S, Peng W, Williamson SD, Banazadeh A, Torres Ulloa KY, Mechref Y, Advances in mass spectrometry based glycomics, Electrophoresis 39(24) (2018) 3063–3081. [PubMed: 30199110]

[48]. Ruhaak LR, Xu G, Li Q, Goonatilleke E, Lebrilla CB, Mass spectrometry approaches to glycomic and glycoproteomic analyses, Chemical Reviews 118(17) (2018) 7886–7930. [PubMed: 29553244]

[49]. Angel PM, Bayoumi AS, Hinton RB, Ru YS, Bichell D, Mayer JE, Scott HB, Caprioli RM, MALDI Imaging Mass Spectrometry as a Lipidomic Approach to Heart Valve Research, The Journal of Heart Valve Disease 25(2) (2016) 240–252. [PubMed: 27989075]

[50]. Angel PM, Caprioli RM, Matrix-assisted laser desorption ionization imaging mass spectrometry: in situ molecular mapping, Biochemistry 52(22) (2013) 3818–3828. PMID:23259809. [PubMed: 23259809]

[51]. Norris JL, Caprioli RM, Analysis of tissue specimens by matrix-assisted laser desorption/ionization imaging mass spectrometry in biological and clinical research, Chemical Reviews 113(4) (2013) 2309–2342. PMCID: PMC3624074. [PubMed: 23394164]

Author Manuscript Author Manuscript Author Manuscript Author Manuscript

[52]. West CA, Drake RR, Mehta AS, Enzymatic Approach to Distinguish Fucosylation Isomers of N-linked Glycans in Tissues Using MALDI Imaging Mass Spectrometry., Journal of Proteome Research in press. (2020).

[53]. Drake RR, Powers TW, Norris Caneda K, Mehta AS, Angel PM, In Situ Imaging of N Glycans by MALDI Imaging Mass Spectrometry of Fresh or Formalin Fixed Paraffin Embedded Tissue, Current Protocols in Protein Science 94(1) (2018) e68. [PubMed: 30074304]

[54]. Powers TW, Jones EE, Betesh LR, Romano PR, Gao P, Copland JA, Mehta AS, Drake RR, Matrix assisted laser desorption ionization imaging mass spectrometry workflow for spatial profiling analysis of N-linked glycan expression in tissues, Analytical Chemistry 85(20) (2013) 9799–9806. PMID: 24050758. [PubMed: 24050758]

[55]. Tarentino AL, Quinones G, Plummer TH Jr, Overexpression and purification of non-glycosylated recombinant endo-β-N-acetylglucosaminidase F3, Glycobiology 5(6) (1995) 599–601. [PubMed: 8563147]

[56]. Clift C, Drake RR, Mehta AS, Angel PM, Comparative 2D N-glycome, Stromal Peptide, and Tryptic Peptide Mapping from the Same FFPE Tissue Section using MALDI Imaging Mass Spectrometry, in: Presentation P. (Ed.) Second Annual Imaging MAss Spectrometry Conference., Charleston, SC, 2018.

[57]. Holst S, Heijs B, de Haan N, van Zeijl RJM, Briaire-de Bruijn IH, van Pelt GW, Mehta AS, Angel PM, Mesker WE, Tollenaar RAEM, Linkage-specific in-situ sialic acid derivatization for N-glycan mass spectrometry imaging of FFPE tissues, Analytical Chemistry 88(11) (2016) 5904–5913. [PubMed: 27145236]

[58]. Damerell D, Ceroni A, Maass K, Ranzinger R, Dell A, Haslam SM, Annotation of Glycomics MS and MS/MS Spectra Using the GlycoWorkbench Software Tool, in: Lutteke T, Frank M. (Eds.), Method in Molecular Biology, Springer, Springer, 2015, pp. 3–15. PMID: 25753699.

[59]. Saeed AI, Bhagabati NK, Braisted JC, Liang W, Sharov V, Howe EA, Li J, Thiagarajan M, White JA, Quackenbush J, TM4 Microarray Software Suite, Methods in Enzymology 411 (2006) 134–193. PMID: 16939790. [PubMed: 16939790]

[60]. Metsalu T, Vilo J, ClustVis: a web tool for visualizing clustering of multivariate data using Principal Component Analysis and heatmap, Nucleic Acids Research 43(W1) (2015) W566–W570. [PubMed: 25969447]

[61]. Trapnell C, Pachter L, Salzberg SL, TopHat: discovering splice junctions with RNA-Seq, Bioinformatics 25(9) (2009) 1105–1111. PMID:19289445, PMCID:PMC2672628. [PubMed: 19289445]

[62]. Davis-Turak J, Courtney SM, Hazard ES, Glen WB Jr., da Silveira WA, Wesselman T, Harbin LP, Wolf BJ, Chung D, Hardiman G, Genomics pipelines and data integration: challenges and opportunities in the research setting, Expert Rev Mol Diagn 17(3) (2017) 225–237. [PubMed: 28092471]

[63]. Love MI, Huber W, Anders S, Moderated estimation of fold change and dispersion for RNA-seq data with DESeq2, Genome Biol 15(12) (2014) 550. [PubMed: 25516281]

[64]. Dobin A, Davis CA, Schlesinger F, Drenkow J, Zaleski C, Jha S, Batut P, Chaisson M, Gingeras TR, STAR: ultrafast universal RNA-seq aligner, Bioinformatics 29(1) (2013) 15–21. [PubMed: 23104886]

[65]. Benjamini Y, Hochberg Y, Controlling the false discovery rate: a practical and powerful approach to multiple testing, Journal of the Royal Statistical Society. Series B (Methodological) 57(1) (1995) 289–300.

[66]. Rini J, Esko JD, Chapter 6: Glycosyltransferases and Glycan-processing enzymes. Essentials of Glycobiology. Varki A, Cummings RD, Esko JD, et al., editors, in: VArki A, Cummings RD, Esko JD (Ed.), Essentials of Glycobiology 3rd edition, Cold Spring Harbor: Cold Spring Harbor Laboratory Press, NY, 2017.

[67]. Powers TW, Neely BA, Shao Y, Tang H, Troyer DA, Mehta AS, Haab BB, Drake RR, MALDI imaging mass spectrometry profiling of N-glycans in formalin-fixed paraffin embedded clinical tissue blocks and tissue microarrays, PLoS One 9(9) (2014) e106255, pp1–11. PMID: 25184632.

Author Manuscript Author Manuscript Author Manuscript Author Manuscript

[68]. Drake RR, Powers TW, Norris Caneda K, Mehta AS, Angel PM, In Situ Imaging of N Glycans by MALDI Imaging Mass Spectrometry of Fresh or Formalin Fixed Paraffin Embedded Tissue, Current Protocols in Protein Science 94(1) (2018) e68. PMID: 30074304. [PubMed: 30074304]

[69]. De Leoz MLA, Young LJT, An HJ, Kronewitter SR, Kim J, Miyamoto S, Borowsky AD, Chew HK, Lebrilla CB, High-mannose glycans are elevated during breast cancer progression, Molecular & Cellular Proteomics 10(1) (2011) M110–002717.PMCID: PMC3013453.

[70]. An HJ, Kronewitter SR, de Leoz MLA, Lebrilla CB, Glycomics and disease markers, Current Opinion in Chemical Biology 13(5–6) (2009) 601–607. [PubMed: 19775929]

[71]. Hedlund M, Ng E, Varki A, Varki NM, α2–6–Linked sialic acids on N-glycans modulate carcinoma differentiation in vivo, Cancer Research 68(2) (2008) 388–394. PMID: 18199532. [PubMed: 18199532]

[72]. Varki A, Sialic acids in human health and disease, Trends in Molecular Medicine 14(8) (2008) 351–360. [PubMed: 18606570]

[73]. Varki A, Gagneux P, Multifarious roles of sialic acids in immunity, Annals of the New York Academy of Sciences 1253(1) (2012) 16. [PubMed: 22524423]

[74]. Yu Z, Lai C-M, Maoui M, Banville D, Shen S-H, Identification and characterization of S2V, a novel putative siglec that contains two V set Ig-like domains and recruits protein-tyrosine phosphatases SHPs, J Biol Chem 276(26) (2001) 23816–23824. [PubMed: 11328818]

[75]. Mitra N, Banda K, Altheide TK, Schaffer L, Johnson-Pais TL, Beuten J, Leach RJ, Angata T, Varki N, Varki A, SIGLEC12, a human-specific segregating (pseudo) gene, encodes a signaling molecule expressed in prostate carcinomas, J Biol Chem 286(26) (2011) 23003–23011. [PubMed: 21555517]

[76]. Lackie PM, Zuber C, Roth J, Expression of polysialylated N-CAM during rat heart development, Differentiation 47(2) (1991) 85–98. [PubMed: 1955110]

[77]. Wiltz D, Arevalos CA, Balaoing LR, Blancas AA, Sapp MC, Zhang X, Grande-Allen KJ, Extracellular matrix organization, structure, and function, in: Aikawa E. (Ed.), Calcific Aortic Valve Disease, InTech2013.

[78]. Rodriguez KJ, Piechura LM, Masters KS, Regulation of valvular interstitial cell phenotype and function by hyaluronic acid in 2-D and 3-D culture environments, Matrix Biology 30(1) (2011) 70–82. [PubMed: 20884350]

[79]. Liu AC, Joag VR, Gotlieb AI, The emerging role of valve interstitial cell phenotypes in regulating heart valve pathobiology, American Journal of Pathology 171(5) (2007) 1407–1418. PMCID: PMC2043503.

[80]. Ohtsubo K, Marth JD, Glycosylation in cellular mechanisms of health and disease, Cell 126(5) (2006) 855–867. [PubMed: 16959566]

[81]. Reily C, Stewart TJ, Renfrow MB, Novak J, Glycosylation in health and disease, Nature Reviews Nephrology (2019) 1.

[82]. Ryczko MC, Pawling J, Chen R, Rahman AMA, Yau K, Copeland JK, Zhang C, Surendra A, Guttman DS, Figeys D, Metabolic reprogramming by hexosamine biosynthetic and golgi N-Glycan branching pathways, Scientific reports 6 (2016) 23043. PMID: 26972830. [PubMed: 26972830]

[83]. Lucena MC, Carvalho-Cruz P, Donadio JL, Oliveira IA, de Queiroz RM, Marinho-Carvalho MM, Sola-Penna M, de Paula IF, Gondim KC, McComb ME, Epithelial mesenchymal transition induces aberrant glycosylation through hexosamine biosynthetic pathway activation, J Biol Chem 291(25) (2016) 12917–12929. PMCID: PMC4933211. [PubMed: 27129262]

[84]. Taparra K, Tran PT, Zachara NE, Hijacking the hexosamine biosynthetic pathway to promote EMT-mediated neoplastic phenotypes, Frontiers in Oncology 6 (2016) 85.PMID: 27148477. [PubMed: 27148477]

[85]. Marques-da-Silva D, Francisco R, Webster D, dos Reis Ferreira V, Jaeken J, Pulinilkunnil T, Cardiac complications of congenital disorders of glycosylation (CDG): a systematic review of the literature, Journal of Inherited Metabolic Disease 40(5) (2017) 657–672. [PubMed: 28726068]

[86]. Becker DJ, Lowe JB, Fucose: biosynthesis and biological function in mammals, Glycobiology 13(7) (2003) 41R–53R. PMID: 12651883.

Author Manuscript Author Manuscript Author Manuscript Author Manuscript

[87]. Schachter H, The search for glycan function: Fucosylation of the TGF-β1 receptor is required for receptor activation, Proceedings of the National Academy of Sciences of the United States of America 102(44) (2005) 15721–15722. PMCID: PMC1276088. [PubMed: 16249330]

[88]. Haines N, Irvine KD, Glycosylation regulates Notch signalling, Nature Reviews Molecular Cell Biology 4(10) (2003) 786–797. [PubMed: 14570055]

[89]. Mehta A, Comunale MA, Rawat S, Casciano JC, Lamontagne J, Herrera H, Ramanathan A, Betesh L, Wang M, Norton P, Intrinsic hepatocyte dedifferentiation is accompanied by upregulation of mesenchymal markers, protein sialylation and core alpha 1, 6 linked fucosylation, Scientific reports 6 (2016) 27965.PMCID: PMC4916422. [PubMed: 27328854]

[90]. Norton PA, Comunale MA, Krakover J, Rodemich L, Pirog N, D'Amelio A, Philip R, Mehta AS, Block TM, N-linked glycosylation of the liver cancer biomarker GP73, J Cell Biochem 104(1) (2008) 136–49. [PubMed: 18004786]

[91]. Miyoshi E, Nakano M, Fucosylated haptoglobin is a novel marker for pancreatic cancer: detailed analyses of oligosaccharide structures, Proteomics 8(16) (2008) 3257–62. [PubMed: 18646007]

[92]. Chen C-Y, Jan Y-H, Juan Y-H, Yang C-J, Huang M-S, Yu C-J, Yang P-C, Hsiao M, Hsu T-L, Wong CH, Fucosyltransferase 8 as a functional regulator of nonsmall cell lung cancer, Proceedings of the National Academy of Sciences 110(2) (2013) 630–635.

[93]. Shao K, Chen ZY, Gautam S, Deng NH, Zhou Y, Wu XZ, Posttranslational modification of Ecadherin by core fucosylation regulates Src activation and induces epithelial–mesenchymal transition-like process in lung cancer cells, Glycobiology 26(2) (2016) 142–154. [PubMed: 26443198]

[94]. Tu C-F, Wu M-Y, Lin Y-C, Kannagi R, Yang R-B, FUT8 promotes breast cancer cell invasiveness by remodeling TGF-β receptor core fucosylation, Breast Cancer Research 19(1) (2017) 111. [PubMed: 28982386]

[95]. Li J, Hsu H-C, Mountz JD, Allen JG, Unmasking fucosylation: from cell adhesion to immune system regulation and diseases, Cell Chemical Biology 25(5) (2018) 499–512. [PubMed: 29526711]

[96]. Miyoshi E, Moriwaki K, Terao N, Tan C-C, Terao M, Nakagawa T, Matsumoto H, Shinzaki S, Kamada Y, Fucosylation is a promising target for cancer diagnosis and therapy, Biomolecules 2(1) (2012) 34–45. [PubMed: 24970126]

[97]. Liang W, Mao S, Sun S, Li M, Li Z, Yu R, Ma T, Gu J, Zhang J, Taniguchi N, Core fucosylation of the T cell receptor is required for T cell activation, Frontiers in Immunology 9 (2018) 78. [PubMed: 29434598]

[98]. Varki A, Cummings BS, Esko JD, Chapter 14: Sialic Acids, in: Varki A, Cummings RD, Esko JD, Freeze HH, Stanley P, Bertozzi CR, Hart GW, Etzler ME (Eds.) Essentials of Glycobiology. 2nd edition., Cold Spring Harbor (NY), 2009.

[99]. Schwarzkopf M, Knobeloch K-P, Rohde E, Hinderlich S, Wiechens N, Lucka L, Horak I, Reutter W, Horstkorte R, Sialylation is essential for early development in mice, Proceedings of the National Academy of Sciences 99(8) (2002) 5267–5270.

[100]. Abeln M, Albers I, Peters-Bernard U, Flächsig-Schulz K, Kats E, Kispert A, Tomlinson S, Gerardy-Schahn R, Münster-Kühnel A, Weinhold B, Sialic acid is a critical fetal defense against maternal complement attack, The Journal of Clinical Investigation 129(1) (2019) 422–436. [PubMed: 30382946]

[101]. Scott DW, Vallejo MO, Patel RP, Heterogenic endothelial responses to inflammation: role for differential N glycosylation and vascular bed of origin, Journal of the American Heart Association 2(4) (2013) e000263.

[102]. Vajaria BN, Patel KR, Begum R, Patel PS, Sialylation: an avenue to target cancer cells, Pathology & Oncology Research 22(3) (2016) 443–447. [PubMed: 26685886]

[103]. Garnham R, Scott E, Livermore KE, Munkley J, ST6GAL1: A key player in cancer, Oncology Letters 18(2) (2019) 983–989. [PubMed: 31423157]

[104]. Hinton RB, Yutzey KE, Heart Valve Structure and Function in Development and Disease, Annual review of physiology 73 (2011) 29–46. PMCID: PMC4209403.

[105]. Bennett ES, Deng W, Qi J, The Sialyltransferase, ST3Gal4, Protects Against Pressure-Induced Cardiac Hypertrophy, Federation of American Societies for Experimental Biology, 2013.

Author Manuscript Author Manuscript Author Manuscript Author Manuscript

[106]. Lackie PM, Zuber C, Roth J, Polysialic acid of the neural cell adhesion molecule (N-CAM) is widely expressed during organogenesis in mesodermal and endodermal derivatives, Differentiation 57(2) (1994) 119131.

[107]. Crocker PR, Paulson JC, Varki A, Siglecs and their roles in the immune system, Nature Reviews Immunology 7(4) (2007) 255–266.

[108]. Macauley MS, Crocker PR, Paulson JC, Siglec-mediated regulation of immune cell function in disease, Nature Reviews Immunology 14(10) (2014) 653–666.

[109]. Lübbers J, Rodríguez E, Van Kooyk Y, Modulation of immune tolerance via Siglec-sialic acid interactions, Frontiers in Immunology 9 (2018) 2807. [PubMed: 30581432]

[110]. Angata T, Varki NM, Varki A, A second uniquely human mutation affecting sialic acid biology, J Biol Chem 276(43) (2001) 40282–40287. [PubMed: 11546777]

[111]. Scott DW, Patel RP, Endothelial heterogeneity and adhesion molecules N-glycosylation: implications in leukocyte trafficking in inflammation, Glycobiology 23(6) (2013) 622–633. [PubMed: 23445551]

[112]. Chiu J-J, Lee P-L, Chen C-N, Lee C-I, Chang S-F, Chen L-J, Lien S-C, Ko Y-C, Usami S, Chien S, Shear stress increases ICAM-1 and decreases VCAM-1 and E-selectin expressions induced by tumor necrosis factor-α in endothelial cells, Arteriosclerosis, Thrombosis, and Vascular Biology 24(1) (2004) 73–79.

[113]. Scott DW, Chen J, Chacko BK, Traylor JG Jr, Orr AW, Patel RP, Role of endothelial N-glycan mannose residues in monocyte recruitment during atherogenesis, Arteriosclerosis, Thrombosis, and Vascular Biology 32(8) (2012) e51–e59.

[114]. Marques-da-Silva D, Francisco R, Webster D, dos Reis Ferreira V, Jaeken J, Pulinilkunnil T, Cardiac complications of congenital disorders of glycosylation (CDG): a systematic review of the literature, Journal of Inherited Metabolic Disease 40(5) (2017) 657–672. PMID: 28726068. [PubMed: 28726068]

115. [] Gao C, Ohtsubo K, Gu J, Taniguchi N, 2.7 Biological functions of branched N-glycans related to physiology and pathology of extracellular matrix., in: Karamanos NK (Ed.), Extracellular Matrix: Pathobiology and Signaling, Hubert & Co. GmbH &Co, Germany, 2012.

[116]. Workman JK, Myrick CW, Meyers RL, Bratton SL, Nakagawa TA, Pediatric organ donation and transplantation, Pediatrics 131(6) (2013) e1723–e1730. [PubMed: 23690525]

[117]. Angel PM, Baldwin HS, Gottlieb D, Su YR, Mayer JE, Bichell D, Drake RR, Advances in MALDI Imaging Mass Spectrometry of Proteins in Cardiac Tissue, Including the Heart Valve, Biochimica et Biophysica Acta (BBA)-Proteins and Proteomics 1865(7) (2017) 927–935. PMCID: PMC5527275. [PubMed: 28341601]

[118]. Angel PM, Comte-Walters S, Ball LE, Talbot K, Brockbank KGM, Mehta AS, Drake RR, Mapping Extracellular Matrix Proteins in Formalin-Fixed, Paraffin-embedded Tissues by MALDI Imaging Mass Spectrometry, Journal of Proteome Research 17(1) (2018) 635–646. PMID: 29161047. [PubMed: 29161047]

[119]. Angel PM, Saunders J, Clift CL, White-Gilbertson S, Voelkel-Johnson C, Yeh E, Mehta A, Drake RR, A Rapid Array-Based Approach to N-Glycan Profiling of Cultured Cells, Journal of Proteome Research 18(10) (2019) 3630–3639. [PubMed: 31535553]

[120]. Marquardt T, Denecke J, Congenital disorders of glycosylation: review of their molecular bases, clinical presentations and specific therapies, European Journal of Pediatrics 162(6) (2003) 359–379. [PubMed: 12756558]

[121]. Dwek RA, Butters TD, Platt FM, Zitzmann N, Targeting glycosylation as a therapeutic approach, Nature Reviews Drug Discovery 1(1) (2002) 65–75. [PubMed: 12119611]

Author Manuscript Author Manuscript Author Manuscript Author Manuscript

Highlights

- Pediatric endstage congenital aortic valve stenosis involves unknown regulation of glycosylation
- N-glycans, metabolic sugar codes, are spatially defined in the young valve structure
- Altered N-glycan processing occurs within the disorganized, diseased valve structure
- N-glycans contribute to human aortic valve structure and are disease regulated

Author Manuscript Author Manuscript Author Manuscript Author Manuscript

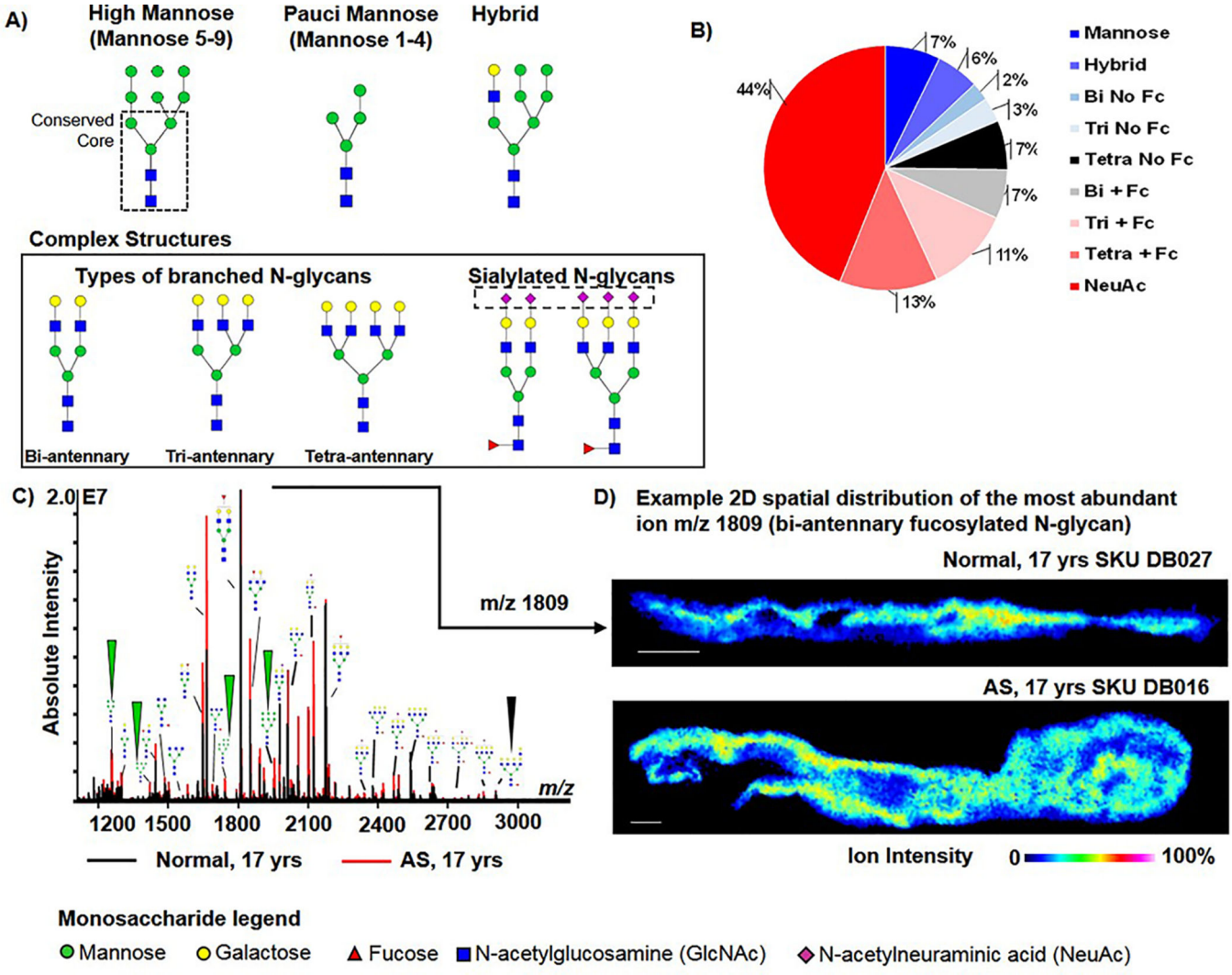

Figure 1. The human aortic valves show complex populations of N-glycans spatially distributed in the aortic valve structure.

A) Representative examples of expected types of N-glycan structures. Far left is the high mannose Man9 N-glycan demonstrating the conserved core (dashed box), common to all N-glycans. Branched N-glycans may have 2–4 branches extending from the core structure. The complex N-glycan structure is a branched structure that may have differing configurations of sialic acids (N-acetylneuraminic acid) and fucose. B) N-glycan composition of the human aortic valve. Bi = biantennary; Tri- tri-antennary; Tetra= tetra-antennary; FC= fucose; NeuAc=N-acetylneuraminic acid. C) Example spectrum from age-matched normal and diseased valve. All N-glycan structure types are represented. Arrows point to mannose N-glycans that are the first structures in N-glycan synthesis. D) Example 2D spatial distribution of the most abundant N-glycan found at mass-to-charge (m/z) 1809 within the age-matched normal and diseased valve. Abbreviations: AS- pediatric endstage congenital aortic valve stenosis.

Author Manuscript Author Manuscript Author Manuscript Author Manuscript

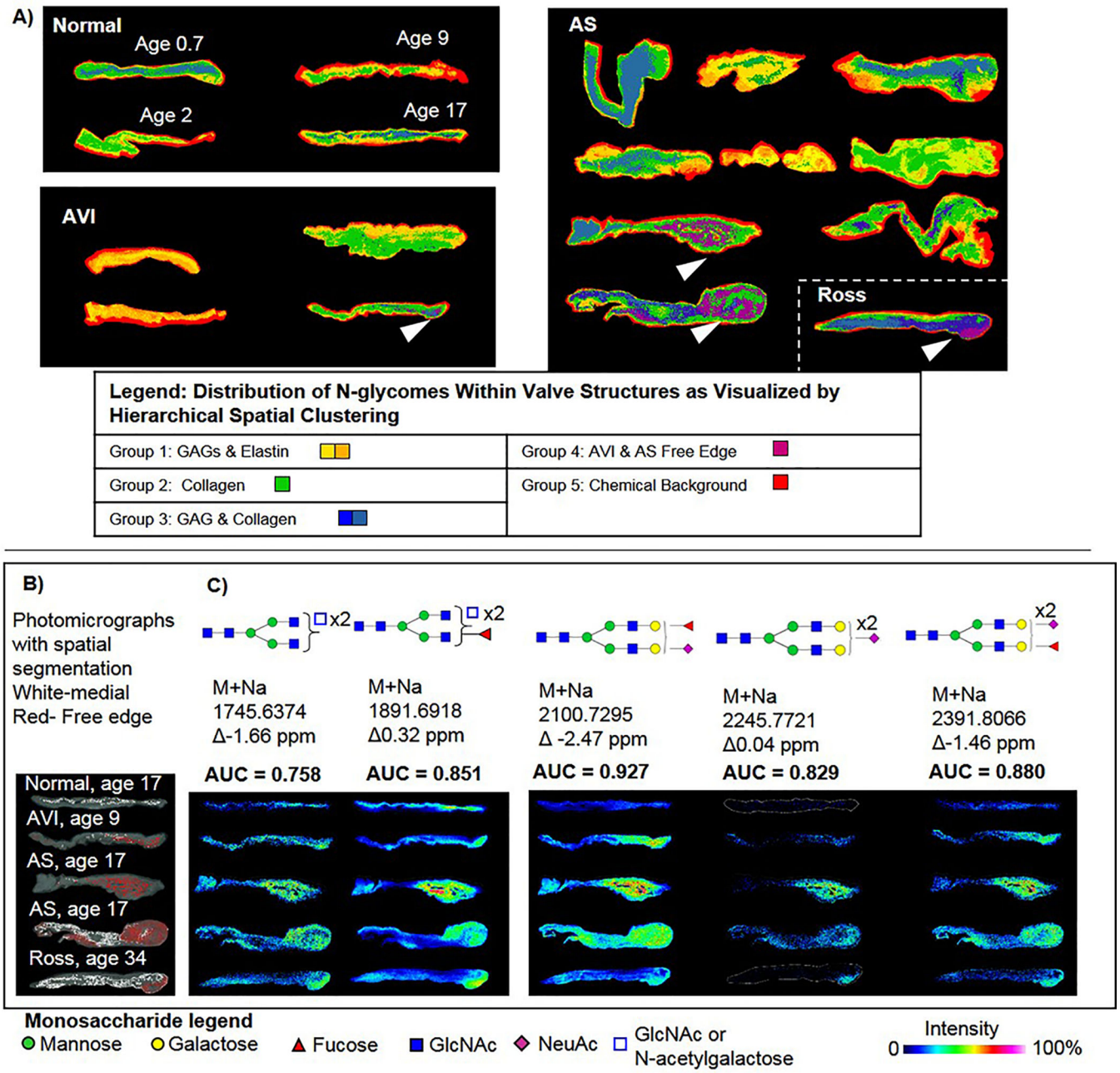

Figure 2. The human AV N-glycome is spatially organized throughout the valve structure.

A) Hierarchical clustering by intensity and localization reports spatial patterns of N-glycan profiles within the human aortic valve. N-glycome clusters are colorized to show the spatial distribution within the valve structure. White arrows highlight unique N-glycomes found within the thickened free edges of some valves. B) Comparison of N-glycomes clustering to medial (white) or distal (red) regions co-registered with photomicrographs of the valve structure. C) Five N-glycans were consistently found increased localized to the thickened free edges. Testing used area under the receiver operating curve (AUC) to determine sensitive and specific discrimination between medial and distal spectra for each

N-glycan structure. Open blue square indicated ambiguity in structure configuration between N-acetylglucosamine and N-acetylgalactosamine, which have identical masses.

Author Manuscript Author Manuscript Author Manuscript Author Manuscript

Author Manuscript Author Manuscript Author Manuscript Author Manuscript

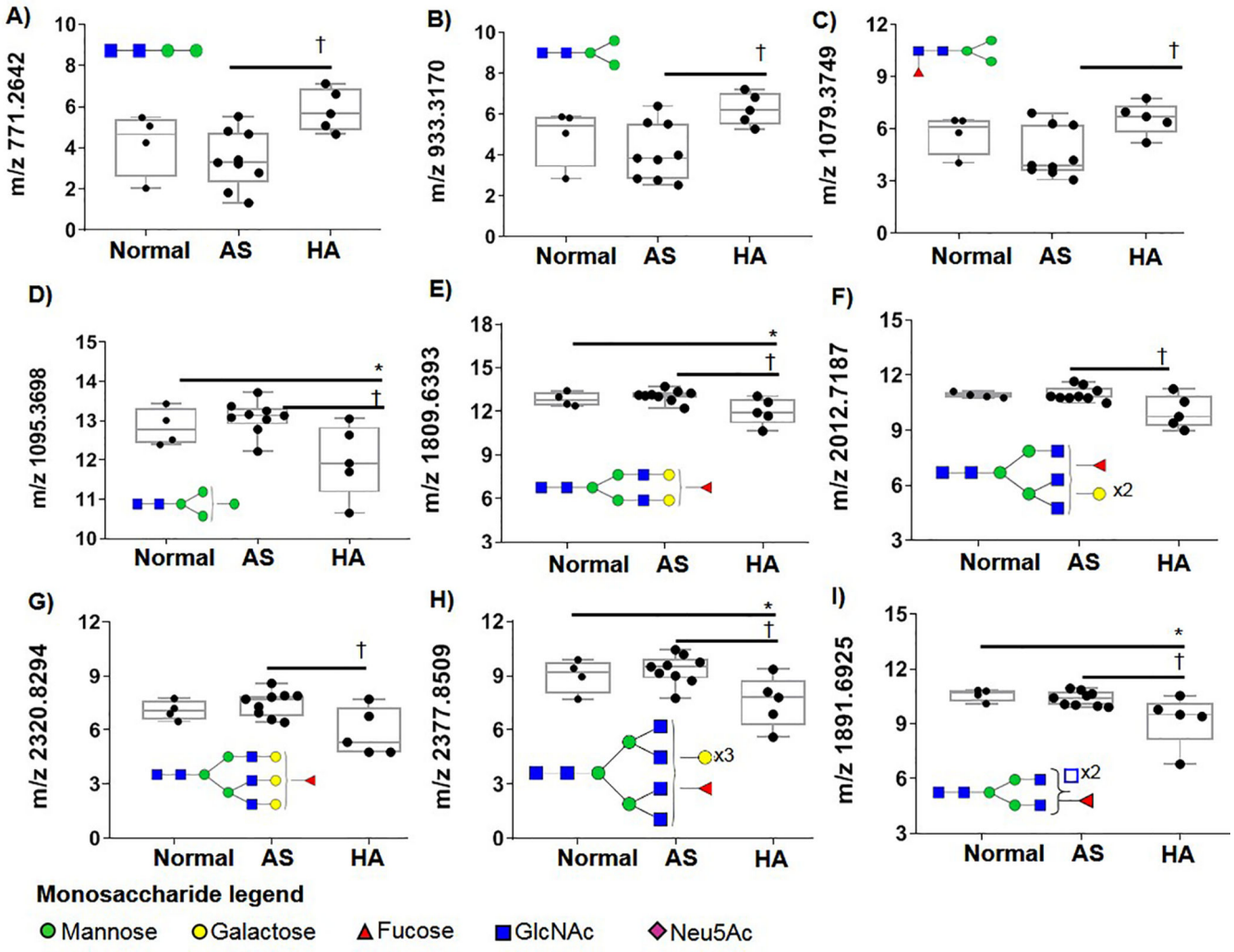

Figure 3. N-glycosylation profiles from hemodynamically altered valves (HA) compared to normal valves or valves with congenital aortic valve stenosis.

Data is natural log of peak intensity normalized by leaflet area. A-C) Paucimannose are elevated in HA valves. D) Man4GlcNAC2 decreases in HA. E-H) a progressive series of single fucosylated bi-antennary, triantennary and tetra-antennary that are decreased in HA. I) HA decreases in the N-glycan m/z 1891. It is possible this could be a tetra-antennary branched structure or have N-acetylgalactosamine residues present. Open blue square indicates ambiguity in structure configuration between N-acetylglucosamine and N-acetylgalactosamine, which have identical masses. * - Mann-Whitney U p-value ≤0.05 compared between normal valve function and AS. † - MWU p-value ≤0.05 compared between AS and HA.

Author Manuscript Author Manuscript Author Manuscript Author Manuscript

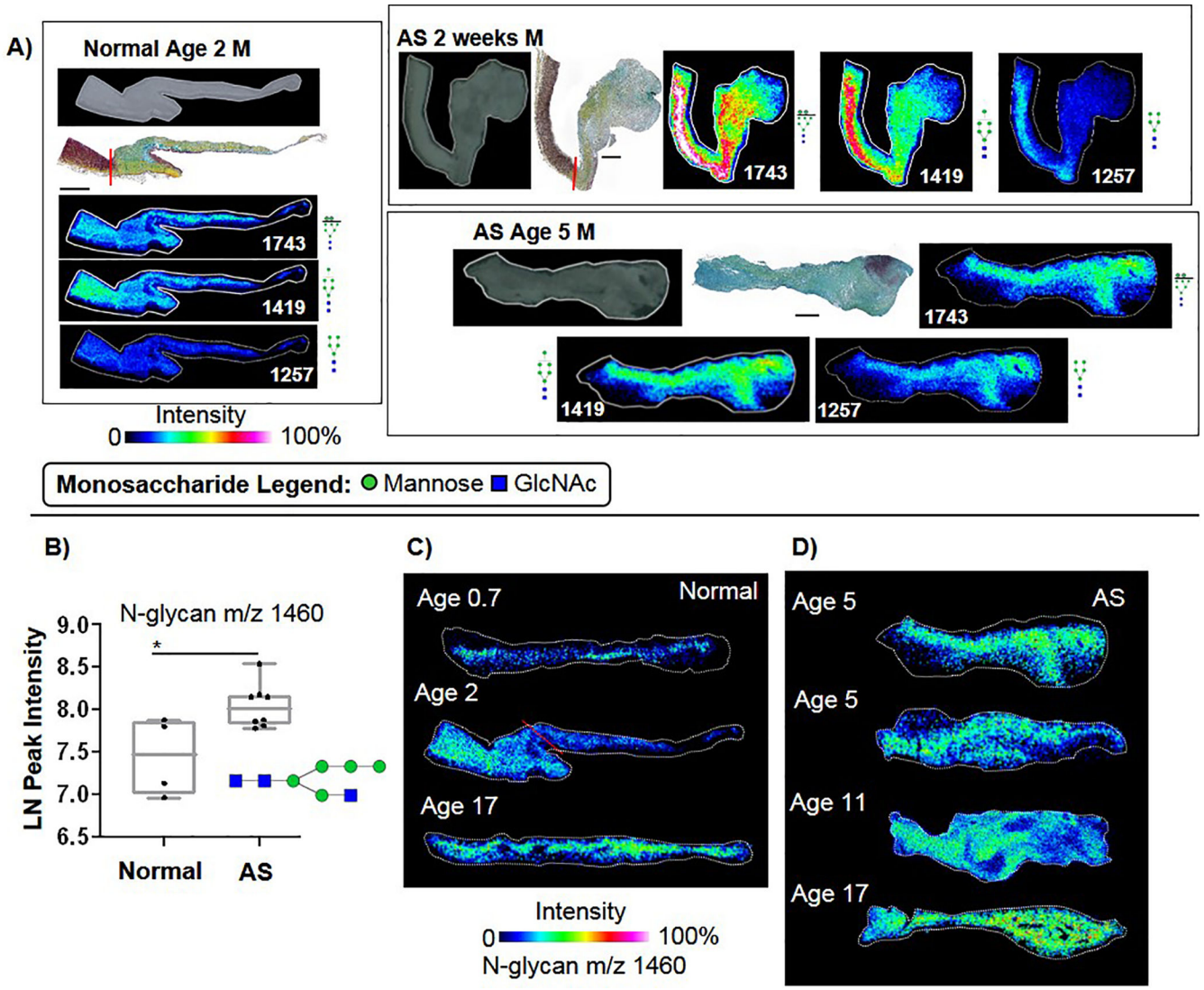

Figure 4. Aortic valve regulation of high mannose N-glycoforms.

A) Example spatial patterns of high mannose structures. Normal aortic valve demonstrates localization to the fibrosa, while AS valves show diffuse expression. Expression extends from the valve to the aorta in AA 2 weeks, appearing with increased intensity in the aorta. B) Hybrid Man5GlcNAc3 (1460) N-glycoform was elevated in AS valves, Mann-Whitney U p-value <0.049. C) Example image patterns of m/z 1460 in normal valves over different pediatric ages. D) Spatial patterns of m/z 1460 in AS valve structures.

Author Manuscript Author Manuscript Author Manuscript Author Manuscript

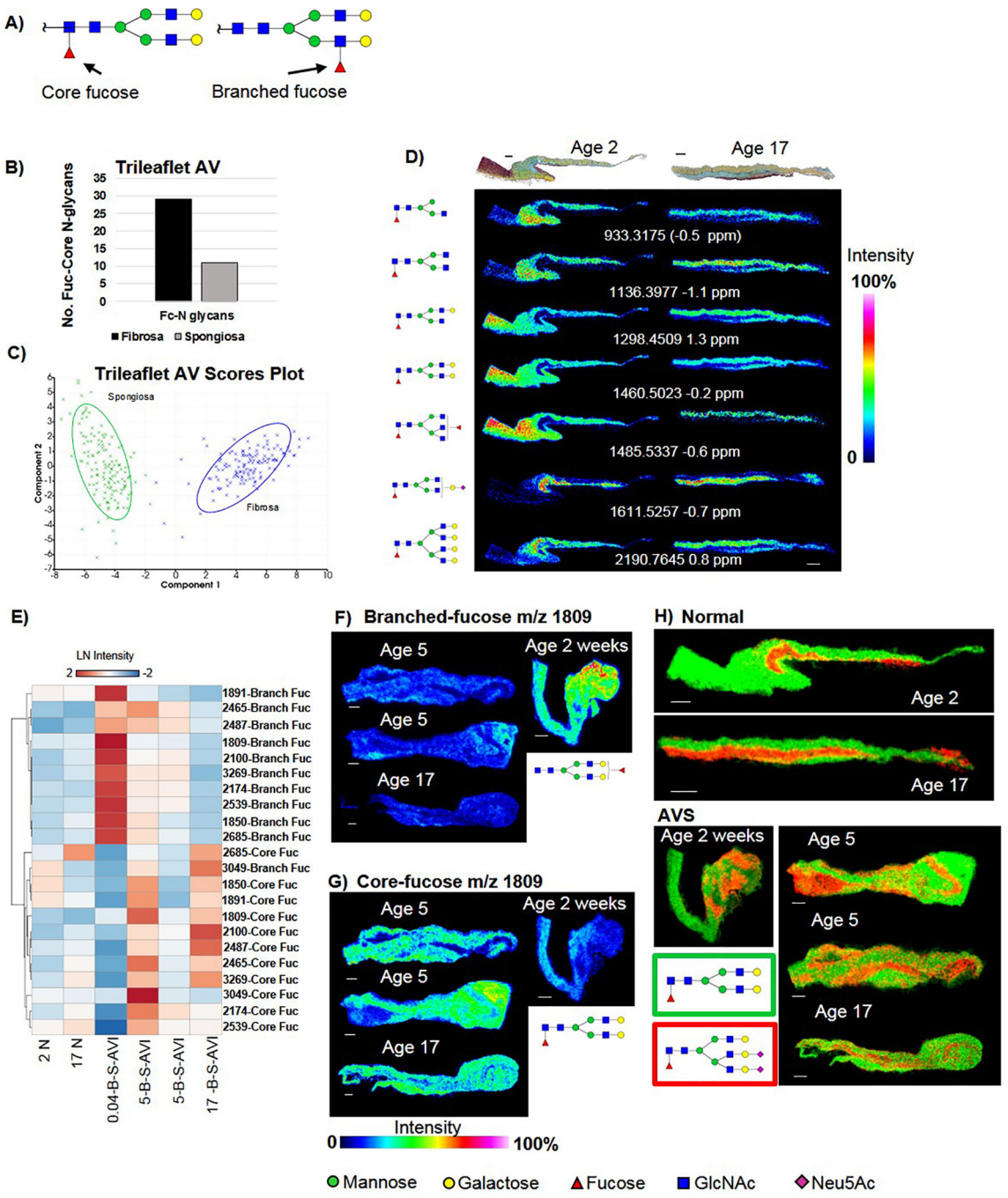

Figure 5. Core fucosylation is the primary fucose configuration of the human aortic valve.

The α1,6 core fucose has been implicated in fibrotic disease patterns. A) Graphical representation of main forms of core versus branched fucosylation in the study. The α1,6 core fucosylation occurs on the first GlcNAc attached to the asparagine residue. The α1,3/4 Branched fucosylation occurs on either of the GlcNAc attached to the core mannose residue. B) Three times more core fucosylated N-glycans were detected in the fibrosa compared to the spongiosa in normal AV tissue. C) By principal component analysis, fucosylated spectra define spongios or fibrosa populations. Component 1 is sample type of Spongiosa or

Author Manuscript Author Manuscript Author Manuscript Author Manuscript

Fibrosa. Component 2 is the magnitude of pixel intensity. D) Patterns of core fucosylation within normal trilayer aortic valves maily follow the fibrosa layer. Mass-charge (m/z) image is the N-glycan minus the core fucose and GlcNAc (−349 Daltons mass difference). E) AS demonstrates a mostly core-fucosylated phenotype. F) Example image patterns of AS tissue with branched fucosylated N-glycan m/z 1809, the most abundant N-glycan in the aortic valve. G) Example of AS image patterns of core-fucosylated N-glycan m/z 1809, the most abundant N-glycan in the aortic valve. H) Very specific core-fucose N-glycans show unique localization in the normal and AS human aortic valve. Note that in AS, the N-glycan localization profiles do not always follow general ECM staining patterns. Bar = 300 μm.

Author Manuscript Author Manuscript Author Manuscript Author Manuscript

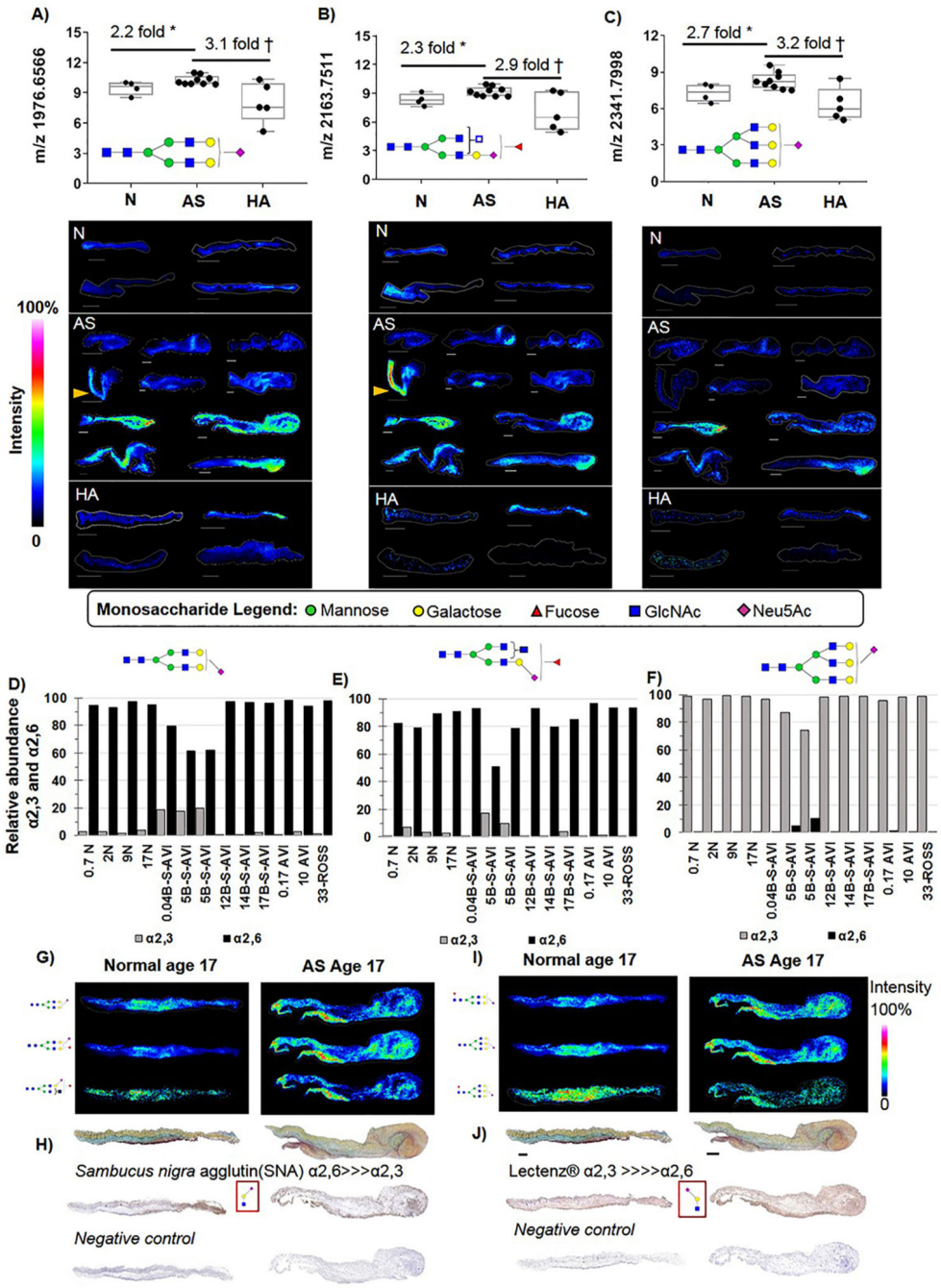

Figure 6. On-tissue measurements of specific Neu5Ac containing N-glycans with consistent elevation in AS expression levels independent of age.

A) Bi-antennary Neu5Ac m/z 1976 is elevated 2.2 fold in AS tissues. Localization is to collagenous regions of the leaflet. B) Putative tri-antennary Neu5Ac m/z 2163 elevated 2.3 fold in AS. A&B) Yellow arrow points to differential spatial expression in aorta versus leaflet, no tused in quantification. C) Tri-antennary Neu5Ac m/z 2341 elevated 2.7 fold in AS. D-F) Linkage analysis of target N-glycans by on-tissue chemical derivatization. The m/z 1976 and 2163 are primarily α2,6 linked while m/z 2341 is primarily α2,3 linked. G) Example image patterns for select α2,6 linked-glycans. H) Lectin staining for the α2,6

NeuAc-galactose-GlcNac motif. I) Example image patterns for select α2,3 linked-glycans. J) Lectin staining for the α2,3 NeuAc-galactose-GlcNac motif. * Two tailed student's t-test p-value ≤0.05; † p-value ≤0.001. Bar= 300 μm.

Author Manuscript Author Manuscript Author Manuscript Author Manuscript

Author Manuscript Author Manuscript Author Manuscript Author Manuscript

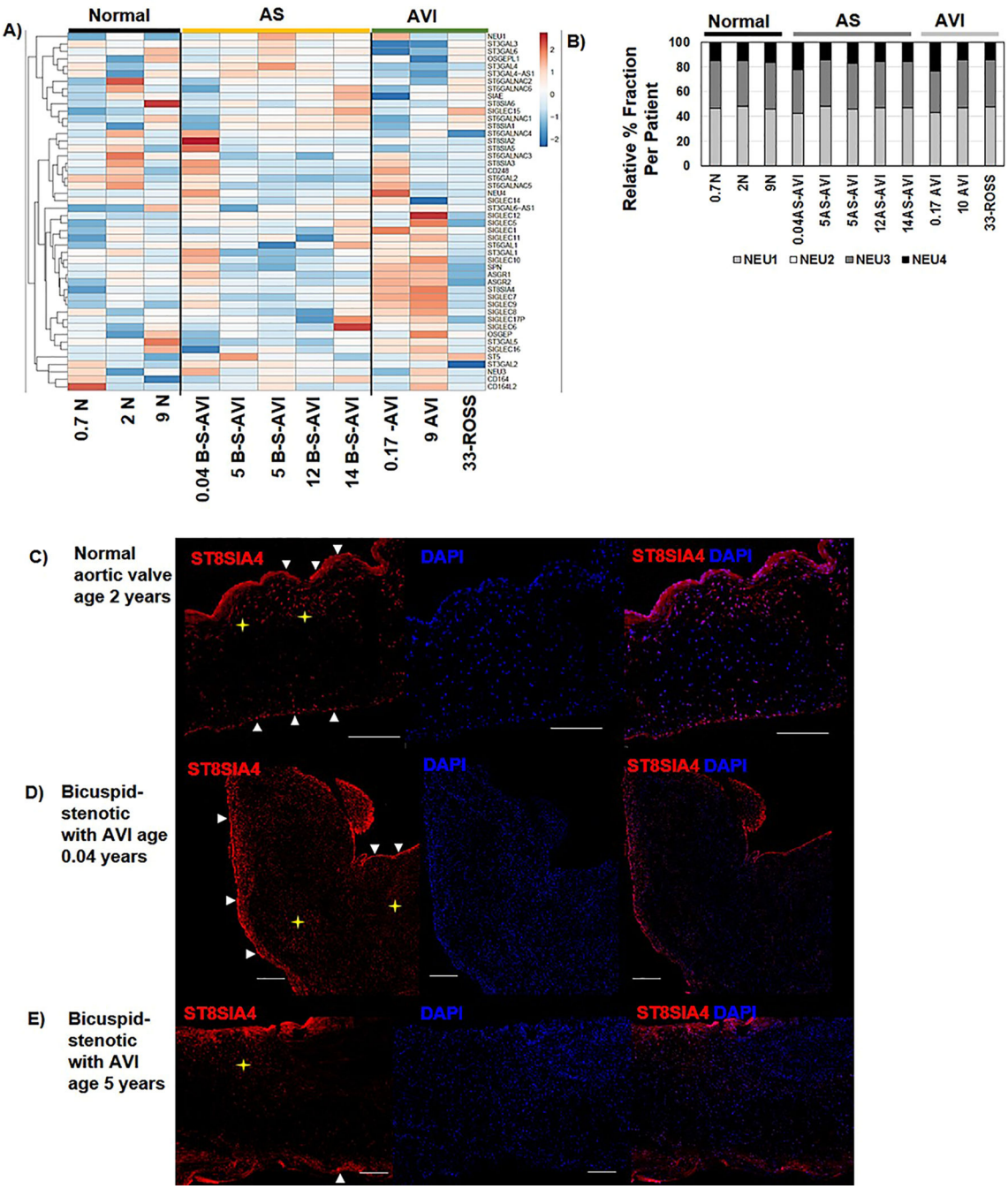

Figure 7. RNA-Seq measurements of sialyltransferases and sialidases.

A) Overall, the human aortic valve shows active regulation of N-glycan sialic acid activity that may be dependent on the individual. B) Neuraminidases, that work on de-sialidation, and localize to different cellular compartments and cell pheontypes show negligible variation among normal or AS valves at the transcriptional level. Neu2 was not detected by RNA-Seq data. C-E) Protein expression of ST8SIA4, which is developmentally regulated in the outflow tract after post-transitional circulation shows localization to the endothelium and fibrosa valvular interstitial cells in normal functioning young valve. In the AS valve

structure expression is found in endothelium and throughout the structure in valvular interstitial cells. Arrows point to endothelium expression. Star highlights internalized expression of ST8SIA4. Bar= 300 μm.

Author Manuscript Author Manuscript Author Manuscript Author Manuscript

Author Manuscript

Author Manuscript

Author Manuscript

Author Manuscript

Table 1.

Glycoenzyme catergories of the study and their target activitybased on [66]. The table reports the glycoenzymes involved in N-glycan synthesis, fucosylation, branching and sialic acid regulation that were a target results of the study. E.R.- endoplasmic reticulum.

Glycoenzyme Category	Activity	Primary Location of Enzyme Activity
Mannosyltransferases	Transfers mannose groups onto the N-glycan precursor	E.R and golgi
Mannosidases	Removes mannose groups off N-glycan structures	cis to medial golgi
Fucosyltransferases	Adds fucose to the N-glycan structure	medial to trans golgi
Fucosidases	Removes fucose from the N-glycan structure	medial to trans golgi
N-acetylglucosaminotransferases	Increases branching of the N-glycan structure	medial to trans
Sialyltransferase	Adds sialic acid to the N-glycan structure	trans-golgi
Sialidases (neuraminidases)	Removes sialic acid from the structure	trans-golgi

Author Manuscript Author Manuscript Author Manuscript Author Manuscript

Table 2.

Clinical characteristics of the cohort. Race/ethnicity: C- Caucasian, L-latino, AA-African-American. Definition of stenosis by 2D echocardiogram (Mean Gradients):Normal Gradient < 5 mmHg; Mild Stenosis 5–25 mmHg; Moderate Stenosis 25–50 mmHg; Severe Stenosis >50 mmHg. N/A- not available.

Normal (N)								
SKU	**Age (Year)**	**Gender**	**Race/ Ethnicity**	**BSA (m^2)**	**Leaflet Morphology**	**Valve Function**	**Left Ventricular Function**	**Primary ECM Phenotype**
DB51	0.66	M	C	0.34	Trileaflet	Normal	Normal	Bilayer
NDRI-1	2	M	L	0.63	Trileaflet	N/A	N/A	Trilayer
DB085	9	F	C	0.95	Trileaflet	Normal	Normal	Trilayer
DB027	17	M	C	2.2	Trileaflet	Normal	Depressed*	Trilayer
Congenital Aortic Valve Stenosis (AS)								
DB106	0.03	M	C	0.21	Bicuspid	Severe Stenosis with AVI	Depressed	GAG
DB040	0.33	M	C	0.37	Bicuspid	Stenosis	Dilated/ severe	GAG
DB105	5	M	C	0.72	Bicuspid	Stenosis with AVI	Normal	GAG
DB119	5	F	-	-	Bicuspid	Moderate Stenosis with AVI	Normal	GAG
DB018	6	F	C	0.70	Bicuspid	Moderate Stenosis with AVI	Normal	Mixed
DB003	11	F	C	1.5	Bicuspid	Moderate Stenosis with AVI	Normal	Mixed
DB117	12	M	-	-	Bicuspid	Moderate Stenosis with AVI	Hyper-dynamic	Elastin
DB041	14	M	C	1.6	Bicuspid	Moderate Stenosis with AVI	Normal	Mixed
DB016	17	M	C	2.1	Bicuspid	Moderate Stenosis with AVI	Normal	Mixed
Hemodynamically Altered (HA)								
DB43	0.13	M	C	0.24	Trileaflet	Moderate subvalvular stenosis with AVI	Markedly depressed	Bilayer
DB114	0.13	F	-	-	N/A	Trivial AVI	Markedly depressed	Bilayer
DB17	0.5	M	L	0.38	N/A	Normal	Markedly depressed	Trilayer
DB083	10	F	AA	1.4	Trileaflet	Trivial AVI	Hypertrophy	Trilayer
DB108	10	F	C	1.3	Trileaflet	Thickened with AVI	Dilated	Mixed
Ross Procedure (pulmonary valve operating in aortic valve position								

Author Manuscript Author Manuscript Author Manuscript Author Manuscript

Normal (N)								
SKU	**Age (Year)**	**Gender**	**Race/ Ethnicity**	**BSA (m^2)**	**Leaflet Morphology**	**Valve Function**	**Left Ventricular Function**	**Primary ECM Phenotype**
DB0102	34	M	C	2.0	Tricuspid	Mild Stenosis	Normal	Mixed

Comparison of Age, BSA, Gender and Race					
	Normal	**AS**	**p-value (AS compared to Normal)**	**HA**	**p-value (HA compared to Normal)**
Age (Years)	7.18; 95% CI [0.17, 14.5]	7.86; 95% CI [4.00, 11.7]	0.969[a]	4.16; 95% CI [0.5, 8.83]	0.389[a]
Body surface area (BSA)	1.03; 95% CI [0.23,1.8)	1.03; 95% CI [0.57,1.5]	0.999[a]	0.83; 95% CI [0.3,1.4]	0.886[a]
Gender (Male/Female)	(3/1)	(6/3)	0.399[b]	(2/3)	0.524[b]
Race/Ethnicity (C/AA/L; Not Reported)	(3/0/1)	(7/0/0; 2NR)	0.185[b]	(2/2/1; 1NR)	0.999[b]

[a] – Mann Whitney U exact p-value;

[b] – two-sided Fisher's exact probability test for proportions.